Linear Quadratic Control for Heavy Duty Vehicle Platooning

KUO-YUN LIANG

KTH Electrical Engineering

Master's Degree Project
Stockholm, Sweden April 2011

XR-EE-RT 2011:017

KTH Electrical Engineering

Linear Quadratic Control for Heavy Duty Vehicle Platooning

KUO-YUN LIANG

Master's Thesis at Automatic Control
Supervisor: Assad Alam
Examiner: Ather Gattami

XR-EE-RT 2011:017

Abstract

Scania CV AB has estimated that the fuel consumption constitutes 30 % of the operational costs of a heavy duty vehicle. With the increasing oil price, reducing the fuel consumption becomes highly profitable. A mitigation to the high fuel consumption is to form a platoon. By introducing vehicle platooning, the fuel consumption is reduced for the following vehicles. The fuel consumption is reduced due to the slipstream effect, which is an atmospheric drag reduction that occurs behind a traveling vehicle. Therefore, by driving the vehicles at a close intermediate distance, the overall resistive force is reduced.

First a study of robustness, of a finite long platoon based upon the string stability criteria, is done. The main focus of this thesis is to find a centralized control law for a finite platoon, which considers the air drag reduction. A LQR and a LQT controller are presented with respect to a given information structure for a three-vehicle platoon. Simulation results show an energy reduction of up to 11.4 % for the second vehicle and up to 13.1 % for the third vehicle, when driving 80 km/h in a platoon on a highway between Södertälje and Norrköping with a time headway of 0.25 s.

Acknowledgements

With this thesis I complete the Master of Science degree in Electrical Engineering at the Royal Institute of Technology (KTH) in Stockholm, Sweden. This work in this master's thesis has been conducted between November 2010 and April 2011 at the Pre-development of Intelligent Transportation Systems Department (REPI) at Scania CV AB in Södertälje, Sweden and was supervised at the Automatic Control Department at KTH.

First, I want to express my deepest gratitude to my supervisor at Scania, Assad Alam, for introducing this project, his valuable time, support, and guidance he has given me throughout the whole project. Henrik Pettersson at Scania is acknowledged for his outstanding help, support, and knowledge that were irreplaceable. I also want to express my gratitude to my supervisor at KTH, Ather Gattami, for the wise inputs and feedback. Many thanks go to everyone at the Pre-development Department, REP, at Scania for welcoming me and making every day enjoyable. Lastly, I want to express my gratitude for the support from family and friends.

Kuo-Yun Liang
Stockholm, 2011

Contents

Part I

Introductory

Chapter 1

Introduction

The commercially available technology in vehicles has grown rapidly in a few years, offering enhanced driving experience and simplifying the daily driving. This development may lead to full automation of the vehicle, enabling everyone to sit behind the wheel without any driving skills. The possibilities can be enormous.

One of the services in progress today for vehicle automation is vehicle platooning. Platooning enables several vehicles to drive with a short intermediate distance in between, acting together as one unit. Platooning serves mainly two purposes, to increase the traffic flow and to reduce the emissions through the reduced fuel consumption. The latter utilizes the atmospheric drag reduction behind a traveling vehicle. It is generally referred to as the slipstream effect, which makes it possible for the following vehicle to consume less fuel.

According to (Schittler, 2003), the average milage per year of an European truck is 150.000 km and has an average fuel consumption of 32.5 l/100 km. Scania CV AB has estimated that the fuel consumption constitutes 30 % of the operational costs of a heavy duty vehicle (HDV) (Scania CV AB, 2001). This means that reducing the fuel consumption can be of vast profit. The fuel consumption can be reduced a lot through HDV platooning with small intermediate distances. Empirical results (Alam et al., 2010) show that the fuel consumption can be reduced up to 7.7 % with a time gap of one second, when two identical HDVs travel as a platoon at 70 km/h.

However, a small distance between vehicles raises issues such as safety and comfort aspects for the driver. Higher risk for collisions is one issue that must be prevented when introducing vehicle platooning. Normally, when an accident occurs on the road, it takes a human driver seconds before reacting and braking, but with vehicle-to-vehicle communication the time delay is reduced tremendously. Therefore, a solution is to introduce vehicle-to-vehicle communication that allows a vehicle to pass on information of its current and next coming behavior to other vehicles in the vicinity.

Chapter 2

Background

2.1 Vehicle platooning

The nomenclature, used in this thesis, for vehicle platooning is defined as shown in fig. 2.1. The platoon consists of $i = \{1, 2, ..., N\}$ vehicles, where $i = 1$ is the lead vehicle of the platoon and $i = N$ is the tail vehicle. v_i denotes the velocity of the ith vehicle and $d_{i-1,i}$ denotes the intermediate distance between the ith vehicle and the vehicle ahead. Furthermore, the movement of the platoon is assumed to be only longitudinal.

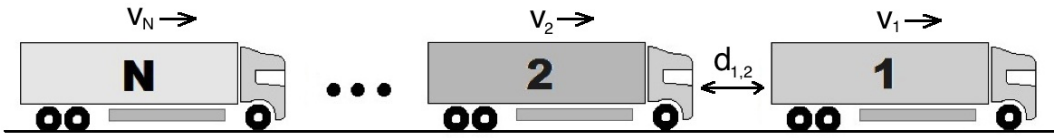

Figure 2.1: Vehicle platooning of N vehicles on a flat road.

2.1.1 Cruise Control and Adaptive intelligent Cruise Control

The Cruise Control (CC), also known as speed control, is a system that automatically maintains the vehicle speed according to the speed reference set by the driver. An extension to the CC is the Adaptive intelligent Cruise Control (AiCC), which takes the vehicle ahead into account. The AiCC will lower its speed to the speed of the vehicle ahead, if the reference speed of the AiCC is set higher than the current speed of the vehicle in front. The distance between the vehicles is the vehicle speed multiplied with a time gap set by the driver, $d_{desire} = \tau_{desire} v$. This is achieved through radar measurements of the velocity and the intermediate distance of the vehicle in front. The AiCC will act as a CC when there is no vehicle within the range of the radar. The experiment in (Alam et al., 2010) utilized the AiCC to accomplish the 7.7 % reduction of fuel consumption for two identical HDVs.

2.1.2 Vehicle-to- vehicle/infrastructure communication

Vehicle-to-vehicle (V2V) and vehicle-to-infrastructure communication (V2I), also known together as V2X communication, allows wider spread of information than the AiCC. V2X communication enables additional information being broadcasted to multiple receivers. With V2V communication, information from several vehicles ahead and the following vehicles can be obtained to make any driving adjustments accordingly. It is also possible to spread its own information and behavior to nearby vehicles. This two-way communication makes it possible for a robust vehicle platooning. V2I communication is a communication between vehicle and infrastructure. It allows the vehicle to gather information such as traffic light or any road work ahead that needs to be considered. This allows smarter path planning, which can be both more time and fuel efficient. In a vehicle platooning with close intermediate distances, the possibilities of time delays, noises, and package losses have to be taken into account such that no collision occurs.

2.2 String stability

One robustness analysis in vehicle platooning is string stability. It is possible that a small change in velocity occurs and amplifies throughout the platoon, this could lead to an unwanted platoon behavior, i.e. a slinky effect, and may result in vehicle collisions. Thus it is of most importance to have a controller that prevents the amplification and propagation. If a platoon has the ability to prevent any slinky effects, it is called string stable. Human drivers in a traffic jam are an example of string instability due to different reactions and time delays, that causes a slinky effect.

The relation between vehicle i and $i-1$ is expressed as:

$$v_i(s) = G_i^v(s)v_{i-1}(s) \tag{2.1}$$

where $G_i^v(s)$ is the velocity transfer function for the ith vehicle. The function describes how the ith vehicle will behave according to the velocity of $i-1$th vehicle. In order to prevent amplification and propagation of velocity changes, the following is defined (Yamamura and Seto, 2006):

$$\|G_i^v(s)\|_\infty \leq 1. \tag{2.2}$$

It is difficult to satisfy eq. (2.2) for every vehicle in a platoon due to non-identical vehicle dynamics and different controllers, thus another approach could be to define:

$$\|G_2^v(s)G_3^v(s)...G_N^v(s)\|_\infty \leq 1 \tag{2.3}$$

It is clear that eq. (2.3) is satisfied when eq. (2.2) is, for all $i \in [2, N]$. Both equations are string stability criteria, however eq. (2.2) is more conservative. Equation (2.2) prevents amplification of velocity change from one vehicle to another. Meanwhile eq. (2.3) assures the tail vehicle does not obtain a disastrous behavior due to a small velocity change from the lead vehicle.

2.3 Related work

The term string stability has been known for the last decades with a large amount of published articles. Articles describing the possibility to stabilize platoons with different strategies and controllers. Variable time headway (Yanakiev and Kanellakopoulos, 1995), obtaining information both from the vehicle ahead and behind (Zhang et al., 1999), and utilizing non-identical decentralized control (Khatir and Davison, 2004) are just three of the many strategies and controls for string stability that have been published. One common factor of these articles is the assumption of identical vehicles in the platoon. Therefore, the first part of this thesis is to analyze the behavior of a platoon with a mass variation.

This thesis is closely related to the master thesis (Hammar and Ovtchinnikov, 2010), where it has taken the air drag reduction into account and performed simulations with different masses. Their work describes a possible strategy to utilize a decentralized controller on a HDV platoon. Hence, this thesis focuses on finding the possibilities with a centralized controller.

2.4 Thesis objective & delimitations

There has been a large amount of research regarding string stability. The authors mainly focus on finding a controller, which allows the vehicle platoon to be string stable. Therefore, one approach in this thesis is to analyze how mass variation can affect string stability of a platoon. This idea came from a spring-mass system where a mass difference causes a damping effect.

Studies of platooning has gotten far with several ideas of how it can be done, especially from the string stability articles. Many suggests a decentralized controller, whereas a centralized control has not been studied further. The AiCC today is a good example of a decentralized controller used commercially. However, there is no commercially available centralized controller. The reason is that there does not exist a standard platform of how it can be obtained. The technology is available but further studies of how communication in platooning should be done and platooning itself need to be done before realizing it. This project has its goal to find a centralized control, which takes the air drag reduction into account and that can be used in platooning. The goal is to analyze the potentials and how well it performs, both in fuel consumption and the ability for maneuvers, compared to a decentralized controller.

This project is divided into two parts, the first part focuses on how mass variations in a platoon affects string stability. Simple dynamics and controller are used to grasp the essential behavior of platooning. This study will mainly focus on mass variations with some simple simulations to verify the results. Meanwhile, the second

part introduces a centralized control that will be simulated using a more realistic vehicle model. The movements of the platoon will be assumed longitudinal due to simplicity and all the information being transferred between vehicles are instantaneous. The only information being broadcasted is the longitudinal position and velocity. No additional functions such as preview information of the road, known as look-ahead, are used. This is to ensure that the focus is on how the platoon behaves and the possibilities of reducing the fuel consumption by utilizing a centralized control. Intruding vehicles and other outer disturbances are neglected.

2.5 Thesis outline

The thesis is structured as followed: chapters 3 and 4 are part II of the thesis, which concerns the string stability study with mass variations. Chapter 3 gives the functions of a simplified platoon and verifies them, meanwhile the following chapter presents a solution to the problem.

Part III concerns the centralized controller. It starts with deriving and describing the vehicle and platoon model of three vehicles thoroughly in chapter 5. This will serve as a premise for all the forthcoming calculations. Chapter 5 also describes a linearization of the non-linear platoon model, since chapter 6 presents an optimal control solution based on a linear model. Chapter 7 shows the results of the simulations based on a Simulink model made by Scania CV AB. A solution to expand the platoon, from a platoon of three vehicles to a larger platoon consisting of sub-platoons, is introduced in chapter 8.

Parts II and III can be read separately, due to the difference in modeling the system. Lastly, chapters 9 to 11 summarize and conclude the whole project along with future possibilities with centralized platooning.

Part II

String stability

Chapter 3

PID-controller

A vehicle platoon can be simplified as a mass-spring-damper system (Yanakiev and Kanellakopoulos, 1996), which this part of study will be using similarly. This study mainly focuses on how a vehicle platoon behaves and how it affects string stability with mass variations using identical control. With the mass-spring system simplification, the vehicle platoon system follows as:

$$m_i\ddot{x}_i + b_i\dot{x}_i = u_i \tag{3.1}$$

where the index i denotes the ith vehicle in the platoon, m_i is the mass, b_i is the damping effect, x_i is the longitudinal position, and u_i is the input of the ith vehicle.

In this chapter, it is assumed that all the vehicles use the same PID-controller but the masses of the vehicles vary. The following PID-controller is used:

$$u_i = P_i(x_{i-1} - x_i - \tau_d\dot{x}_i) + I_i(\int x_{i-1} - x_i - \tau_d\dot{x}_i \,\mathrm{d}t) + D_i(\dot{x}_{i-1} - \dot{x}_i) \tag{3.2}$$

where τ_d denotes the time headway. The index i in the controller will be kept, even if identical controller is used for all vehicles. This makes it easier to distinguish which vehicle the controller belongs to.

3.1 Velocity and relative distance

The first two relations that will be derived are how a velocity change v_{i-1} affects the relative distance $d_{i-1,i} = x_{i-1} - x_i$ and how that distance affects the velocity of the following vehicle, v_i. These two relations will serve as a premise for the forthcoming calculations of the string stability part. The dynamic system is given by inserting eq. (3.1) into eq. (3.2):

$$m_i\ddot{x}_i + b_i\dot{x}_i = P_i(x_{i-1} - x_i - \tau_d\dot{x}_i) + I_i(\int x_{i-1} - x_i - \tau_d\dot{x}_i \,\mathrm{d}t) + D_i(\dot{x}_{i-1} - \dot{x}_i). \tag{3.3}$$

By introducing the following notations $x_{i-1} - x_i = d_{i-1,i}$ and $\dot{x}_i = v_i$, the Laplace transform can be given as:

$$(m_i s + b_i)v_i(s) = (P_i + I_i\frac{1}{s} + D_i s)d_{i-1,i}(s) - (\tau_d P_i + \tau_d I_i\frac{1}{s})v_i(s).$$

The first relation obtained from the calculations is how vehicle i reacts to a change in relative distance $d_{i-1,i}$, which is given by the following transfer function:

$$H_i^{dv}(s) = \frac{v_i(s)}{d_{i-1,i}(s)} = \frac{s^2 D_i + sP_i + I_i}{s^2 m_i + s(b_i + \tau_d P_i) + \tau_d I_i} \tag{3.4}$$

The second relation is how velocity v_{i-1} affects the relative distance $d_{i-1,i}$. This can be obtained with $sd_{i-1,i}(s) = v_{i-1}(s) - v_i(s)$ giving the following transfer function:

$$H_i^{vd}(s) = \frac{d_{i-1,i}(s)}{v_{i-1}(s)} = \frac{s^2 m_i + s(b_i + \tau_d P_i) + \tau_d I_i}{s^3 m_i + s^2(b_i + \tau_d P_i + D_i) + s(P_i + \tau_d I_i) + I_i} \tag{3.5}$$

The steady state error of both transfer functions, eqs. (3.4) and (3.5), are dependent on τ_d, which is reasonable due to which time headway is set by the driver.

3.2 Velocity transfer function

The more important part in a platoon is to analyze how a velocity change affects other vehicles in the platoon. A small velocity change by the lead vehicle should not amplify and propagate throughout the platoon and cause any collisions. By multiplying both the earlier derived transfer functions, eqs. (3.4) and (3.5), the velocity transfer function is obtained:

$$\begin{aligned} G_i^v(s) = \; & H_i^{dv}(s)H_i^{vd}(s) = \frac{v_i(s)}{v_{i-1}(s)} \\ = \; & \frac{s^2 D_i + sP_i + I_i}{s^3 m_i + s^2(b_i + \tau_d P_i + D_i) + s(P_i + \tau_d I_i) + I_i} \end{aligned} \tag{3.6}$$

With eq. (2.2), the string stability criteria is fulfilled when $\|G_i^v(s)\|_\infty \leq 1$. The inequality fulfillment depends mostly on the values of P_i, I_i, and D_i, and somewhat on the mass m_i. This study refers from being dependent on what PID-controller is used, hence eq. (3.6) does not give any insight on how a mass variation affects string stability since it also depends on the PID-controller.

3.3 Relative distance transfer function

Another aspect that should be analyzed in platooning is how a change in relative distance propagates through the platoon. Relative distance between vehicles is a

straightforward answer whether the vehicles collide or not. The transfer function for relative distance can be obtained with the calculation:

$$\begin{aligned} G_i^d(s) &= H_{i-1}^{dv}(s)H_i^{vd}(s) = \frac{d_{i-1,i}(s)}{d_{i-2,i-1}(s)} \\ &= \frac{s^2 m_i + s(b_i + \tau_d P_i) + \tau_d I_i}{s^2 m_{i-1} + s(b_{i-1} + \tau_d P_{i-1}) + \tau_d I_{i-1}} \frac{s^2 D_{i-1} + s P_{i-1} + I_{i-1}}{s^3 m_i + s^2(b_i + \tau_d P_i + D_i) + s(P_i + \tau_d I_i) + I_i}. \end{aligned} \tag{3.7}$$

Notice that the masses of two different vehicles are now included in the transfer function. The first quotient could be simplified due to the identical PID-controller and by doing the following assumptions:

$$\begin{cases} \frac{P_{i-1}}{m_{i-1}} \approx \frac{P_i}{m_i} \\ \frac{b_{i-1}}{m_{i-1}} \approx \frac{b_i}{m_i} \\ \frac{I_{i-1}}{m_{i-1}} \approx \frac{I_i}{m_i}. \end{cases} \tag{3.8}$$

Then eq. (3.7) can be approximated as:

$$G_i^d(s) = \frac{d_{i-1,i}(s)}{d_{i-2,i-1}(s)} \approx \frac{m_i}{m_{i-1}} \frac{s^2 D_{i-1} + s P_{i-1} + I_{i-1}}{s^3 m_i + s^2(b_i + \tau_d P_i + D_i) + s(P_i + \tau_d I_i) + I_i}. \tag{3.9}$$

This approximation clarifies how the platoon should be arranged depending on the vehicle masses. By arranging heavier vehicles first and with a decreasing order in mass, the simplified quotient becomes less than one, $\frac{m_i}{m_{i-1}} < 1$. This enables the eq. (3.9) to satisfy the inequality $\|G_i^d(s)\|_\infty \leq 1$. It should be noted that the inequality could be satisfied with the approximation for eq. (3.9) but may not be satisfied for eq. (3.7). Although the string stability criteria does only include the velocity changes between the vehicles and does not include the amplification and propagation between the relative distances, this area could be as important to study.

3.4 Simulation study I

To verify the result from section 3.3, a small simulation study is made in Matlab. A PID-controller is used and the simulation scenario is a ramp from 0 m/s to 10 m/s in 10 s. To be able to verify the result from eq. (3.9), three different platoon arrangements were used; identical vehicles, increasing weight order, and in decreasing order in mass. To make the three different platoon arrangements comparable, the platoon length and the sum of the weight of all vehicles in the platoon are the same. The reader is referred to appendix A for further information on the simulation setup.

The first simulation is done with a platoon of identical vehicles with the mass of 40 tonnes each. Figure 3.1 illustrates the result with two different platoon lenghts: 41

vehicles in fig. 3.1a and 81 vehicles in fig. 3.1b. The platoon behavior depicted in fig. 3.1 shows a velocity change amplifies throughout the platoon for each vehicle. Furthermore, the relative distance between the vehicles gets influenced, with slinky effect and amplifying distance error as a result. Such conduct is considered string unstable and the H_∞-norm of the velocity transfer function is also above one, see appendix A.

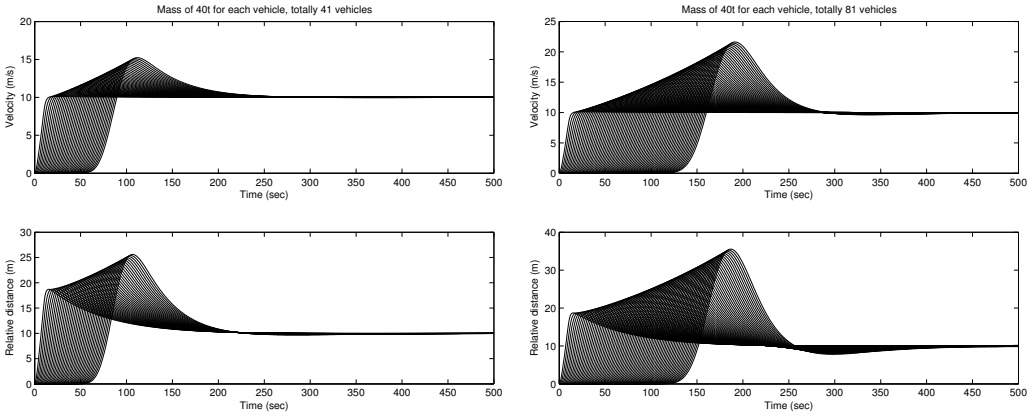

(a) Platoon length of 41 identical vehicles (b) Platoon length of 81 identical vehicles

Figure 3.1: A ramp with identical vehicles of mass 40 tonnes each in a platoon. The velocity and relative distance are plotted.

The second platoon configuration is with weight increasing order. The lead vehicle has a mass of 20 tonnes and the tail vehicle has a weight of 60 tonnes. Two different platoon lengths were simulated, which are presented in fig. 3.2. Figure 3.2a shows the platoon behavior with 41 vehicles with 1000 kg weight gap and fig. 3.2b with 81 vehicles with a weight gap of 500 kg. The results show that the velocity behavior remains growing, similar to the previous simulation, but the major difference is the relative distance. Analysis from eq. (3.9) clearly explains that the H_∞-norm grows with a lighter vehicle in front. This platoon configuration is not considered string stable.

The third and last platoon simulation is a platoon with decreasing order in mass. The mass will remain the same as the second simulation but in reverse order, from 60 tonnes to 20 tonnes. The platoon behavior is depicted in fig. 3.3. Notice that the max velocity is the same for all three platoon configuration. However, the only configuration is the weight decreasing order where the velocity amplification subsides further back in the platoon. The relative distance for the decreasing weight order is highly advantageous over the other platoon configurations. This confirms eq. (3.9), that by arranging heavier vehicles first in a platoon with a descending order the platoon can become string stable. This is with the assumptions that identical controllers are used for every vehicle.

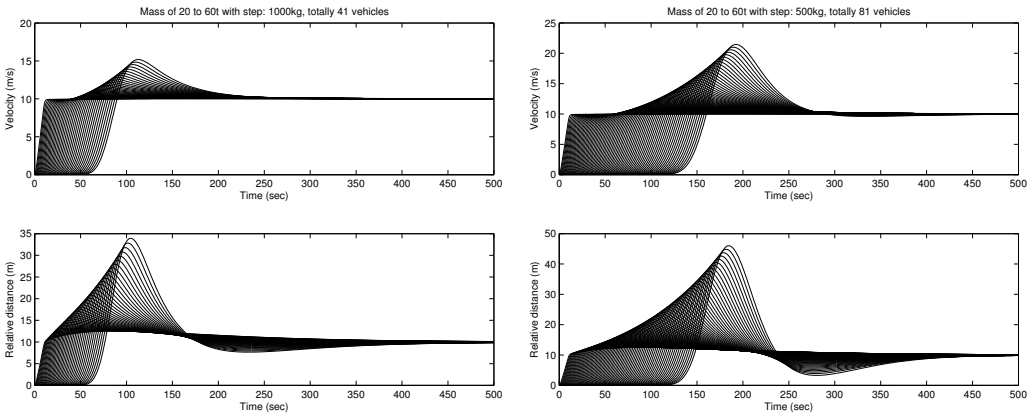

(a) 41 vehicles, weight gap of 1000 kg (b) 81 vehicles, weight gap of 500 kg

Figure 3.2: A ramp with weight increasing platoon order, 20 to 60 tonnes. The velocity and relative distance are plotted.

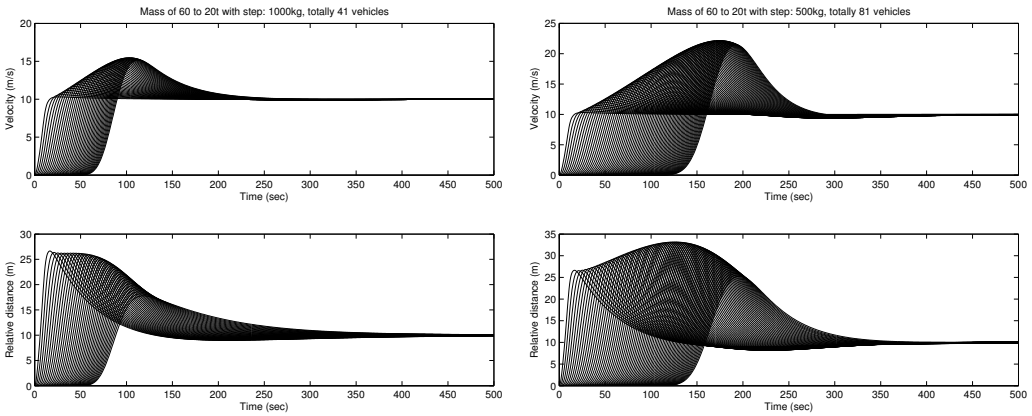

(a) 41 vehicles, weight gap of 1000 kg (b) 81 vehicles, weight gap of 500 kg

Figure 3.3: A ramp with weight decreasing platoon order, 60 to 20 tonnes. The velocity and relative distance are plotted.

Chapter 4

Scaled-varying PID-controller

The problem, with identical controllers in a platoon, is the different dynamics each vehicle has depending on the mass. Each vehicle with different weight has different dynamics and therefore renders identical PID-controller useless for heavier vehicles. A fixed PID-controller is useful for light weighted vehicles up to a point where the controller is no longer considered string stable. A proposed solution is to introduce a scalar to the PID-controller, which can take the mass of the vehicle into account. The vehicle system keeps the same dynamics as in eq. (3.1), meanwhile the proposed controller is now expressed as:

$$u_i = K_i[P_i(x_{i-1} - x_i - \tau_d \dot{x}_i) + I_i(\int x_{i-1} - x_i - \tau_d \dot{x}_i \, \mathrm{d}t) + D_i(\dot{x}_{i-1} - \dot{x}_i)] \quad (4.1)$$

The following sections will follow the same procedure as in chapter 3.

4.1 Transfer functions

The derivations of the four next coming transfer functions are done with exactly the same steps as in sections 3.1 to 3.3, and are therefore omitted in this section. The results of the transfer functions are:

$$\bar{H}_i^{dv}(s) = \frac{v_i(s)}{d_{i-1,1}(s)} = \frac{s^2 D_i + sP_i + I_i}{s^2 \frac{m_i}{K_i} + s(\frac{b_i}{K_i} + \tau_d P_i) + \tau_d I_i} \quad (4.2)$$

$$\bar{H}_i^{vd}(s) = \frac{d_{i-1,i}(s)}{v_{i-1}(s)} = \frac{s^2 \frac{m_i}{K_i} + s(\frac{b_i}{K_i} + \tau_d P_i) + \tau_d I_i}{s^3 \frac{m_i}{K_i} + s^2(\frac{b_i}{K_i} + \tau_d P_i + D_i) + s(P_i + \tau_d I_i) + I_i} \quad (4.3)$$

$$\bar{G}_i^{v}(s) = \frac{v_i(s)}{v_{i-1}(s)} = \frac{s^2 D_i + sP_i + I_i}{s^3 \frac{m_i}{K_i} + s^2(\frac{b_i}{K_i} + \tau_d P_i + D_i) + s(P_i + \tau_d I_i) + I_i} \quad (4.4)$$

$$\bar{G}_i^{d}(s) = \frac{d_{i-1,i}(s)}{d_{i-2,i-1}(s)} \approx \frac{m_i}{m_{i-1}} \frac{K_{i-1}}{K_i} \frac{s^2 D_{i-1} + sP_{i-1} + I_{i-1}}{s^3 \frac{m_i}{K_i} + s^2(\frac{b_i}{K_i} + \tau_d P_i + D_i) + s(P_i + \tau_d I_i) + I_i} \quad (4.5)$$

Equation (4.5) is an approximation using the following assumptions:

$$\begin{cases} \dfrac{K_{i-1}P_{i-1}}{m_{i-1}} \approx \dfrac{K_iP_i}{m_i} \\ \dfrac{b_{i-1}}{m_{i-1}} \approx \dfrac{b_i}{m_i} \\ \dfrac{K_{i-1}I_{i-1}}{m_{i-1}} \approx \dfrac{K_iI_i}{m_i} \end{cases} \tag{4.6}$$

Similar to chapter 3, eqs. (4.2) to (4.4) do not add further information. The key remains in the relative distance transfer function, eq. (4.5). It is now possible to obtain $\|\bar{G}_i^d(s)\|_\infty \leq 1$ with any kind of mass distribution with the help of the scalars, K_{i-1} and K_i. This was not possible for $G_i^d(s)$ from eq. (3.9), since it was bounded to be arranged in a weight decreasing order to achieve a stable behavior.

4.2 Simulation study II

To validate the results from section 4.1, same simulation from section 3.4 will be done but with a scaled-varying PID-controller. The varying scalar is set to be: $K_i = \frac{m_i}{10000}$. For further information on the simulation setup, the reader is referred to read appendix A.

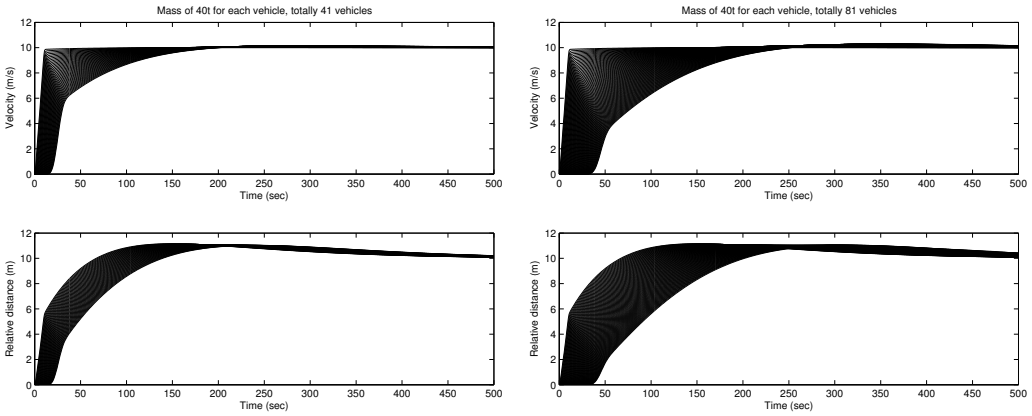

(a) Platoon length of 41 identical vehicles (b) Platoon length of 81 identical vehicles

Figure 4.1: A ramp with identical vehicles using scaled-varying PID. The velocity and relative distance are plotted.

The results of the three different weight distributions are all illustrated in figs. 4.1 to 4.3. The three figures show similar platoon behavior and most importantly, the relative distances between the vehicles do not get amplified or inherit any slinky

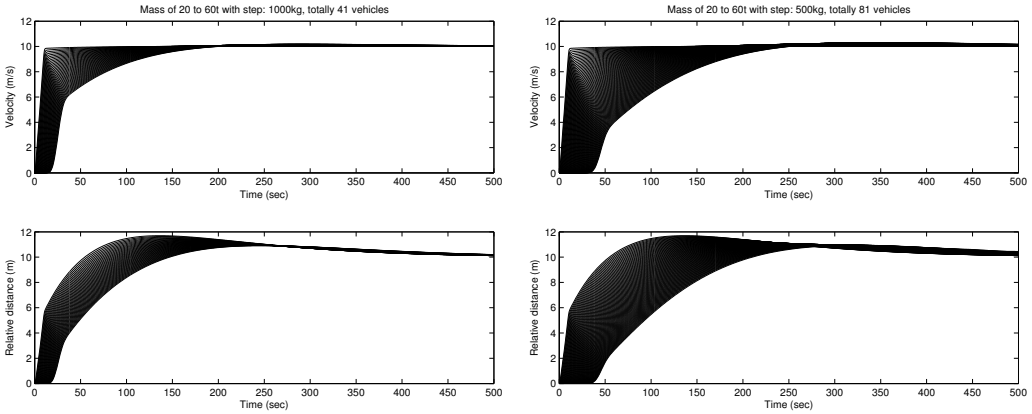

(a) 41 vehicles, weight gap of 1000 kg (b) 81 vehicles, weight gap of 500 kg

Figure 4.2: A ramp with increasing weight order using scaled-varying PID. The velocity and relative distance are plotted.

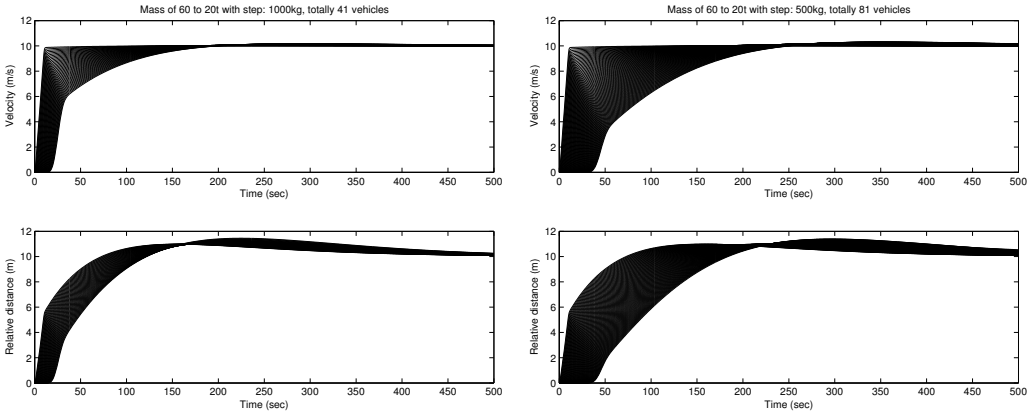

(a) 41 vehicles, weight gap of 1000 kg (b) 81 vehicles, weight gap of 500 kg

Figure 4.3: A ramp with decreasing weight order using scaled-varying PID. The velocity and relative distance are plotted.

effect. This confirms that eq. (4.5) can fulfill the inequality $\|\bar{G}_i^d(s)\| \leq 1$ for any mass distribution. Furthermore, the string stability criteria is also satisfied for all mass variations used in the simulation, i.e. $\|\bar{G}_i^v(s)\| \leq 1$.

Part III

Locally centralized three-vehicle platoon

Chapter 5

Platoon model

To enable an understanding of modeling a HDV platoon, the knowledge of the systems and the dynamics of a HDV are required. The outcome of this chapter is to derive a state-space model of the vehicle model, from the powertrain to the vehicle dynamics of a HDV, with a platoon of three HDVs. This is necessary in order to develop a controller for the platoon. General vehicle modeling can be found in (Gillespie, 1992).

5.1 Powertrain

A basic model of a powertrain with the main parts of interests is depicted in fig. 5.1. The powertrain model follows the same model defined in (Alam, 2008).

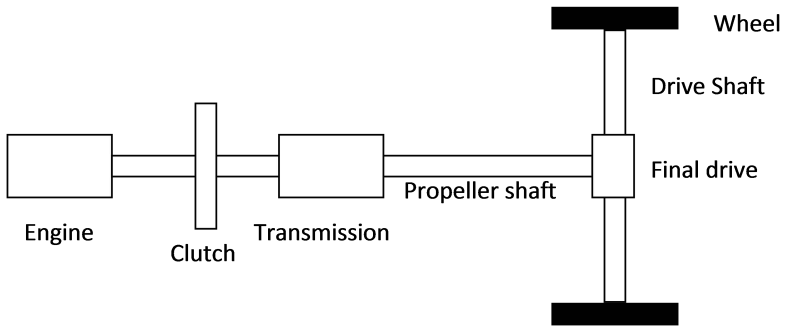

Figure 5.1: A basic model of a powertrain.

Engine

The engine utilized in the model is a diesel engine. The engine output torque, represented as $T_e(\omega_e, \delta_f)$ where ω_e is the angular velocity of the flywheel and δ_f is the fueling level, is characterized by the driving torque, which is produced during combustion, minus internal friction of the engine. The external load comes from the clutch denoted with T_c. Newton's second law of motion gives the following relation:

$$J_e\dot{\omega}_e = T_e - T_c \tag{5.1}$$

where J_e is the mass moment of inertia of the engine.

When the engine works within the operating range, which is ideally between 1100 and 1400 RPM, the torque $T_e(\omega_e, \delta_f)$ can be linearized as:

$$T_e(\omega_e, \delta_f) = k_1\omega_e + k_2\delta_f + k_3 \tag{5.2}$$

where k_1, k_2, and k_3 are constants of the engine properties. The conversion between RPM and angular velocity is:

$$RPM = \frac{60}{2\pi}\omega_e.$$

Clutch

The clutch consists of two frictional discs connecting the flywheel of the engine with the input shaft of the transmission. This type of clutch is mostly found in vehicles equipped with manual transmission. The clutch is considered to be stiff, which yields in no torque and angular velocity change:

$$\begin{aligned} T_t &= T_c \\ \omega_t &= \omega_c \end{aligned} \tag{5.3}$$

where T_t denotes the torque output from the clutch and input to the transmission, and ω_t denotes the angular velocity.

Transmission

The transmission consists of a set of gears that converts the output torque depending on the engaged gear. Each gear has a conversion ratio i_t and an efficiency constant η_t. The inertia is neglected and the gear shifts are assumed to be instantaneous, which results in the following relations:

$$\begin{aligned} T_p &= i_t\eta_t T_t \\ i_t\omega_p &= \omega_e \end{aligned} \tag{5.4}$$

where T_p denotes the output torque from the transmission and input to the propeller shaft, and ω_p denotes the angular velocity.

Propeller shaft

The propeller shaft connects the transmission with the final drive. The shaft is considered to be stiff with no friction, which gives:

$$\begin{aligned} T_f &= T_p \\ \omega_f &= \omega_p \end{aligned} \tag{5.5}$$

where T_p denotes the output torque from the propeller shaft and input to the final drive, and ω_p denotes the angular velocity.

Final drive

The final drive is, like the transmission, characterized by a conversion ratio i_f and an efficiency constant η_f. The inertia is likewise neglected, giving the following relations:

$$\begin{aligned} T_d &= i_f \eta_f T_f \\ i_f \omega_d &= \omega_f \end{aligned} \tag{5.6}$$

where T_d denotes the output torque from the final drive and input to the drive shafts, and ω_d denotes the angular velocity.

Drive shafts

The drive shafts connect the final drive with the wheels. It is presumed that the wheel speed is the same for both wheels and the drive shafts are stiff. Therefore, the powertrain equation is not influenced by the following relations:

$$\begin{aligned} T_w &= T_d \\ \omega_w &= \omega_d \end{aligned} \tag{5.7}$$

where T_w denotes the output torque to the wheels, and ω_w denotes the angular velocity.

Wheels

Lastly, by assuming no slip, the equation of motion for the wheel is described as:

$$J_w \dot{\omega}_w = T_w - T_b - r_w F_w \tag{5.8}$$

$$v = r_w \omega_w = \frac{r_w \omega_e}{i_t i_f} \tag{5.9}$$

where J_w is the wheel inertia, r_w is the wheel radius, v is the vehicle velocity, and F_w is the resulting force that drives the vehicle forward. The braking torque T_b is difficult to model and is therefore neglected in this model.

Complete powertrain

By combining eqs. (5.1) and (5.3) to (5.9) together, the complete powertrain equation can be expressed as:

$$F_w = \frac{i_t i_f \eta_t \eta_f}{r_w} T_e - \frac{J_w + i_t^2 i_f^2 \eta_t \eta_f J_e}{r_w^2} \dot{v} = F_{engine} - F_{inertia} \tag{5.10}$$

where F_{engine} is the force produced from the engine and $F_{inertia}$ is the inner force required for the engine to overcome in order to produce a driving force.

5.2 Longitudinal forces

When a HDV is in motion, there are several forces acting on the vehicle. Figure 5.2 illustrates the longitudinal forces on the HDV. F_{brake} is neglected due to the explanation in previous section, and α denotes the road angle.

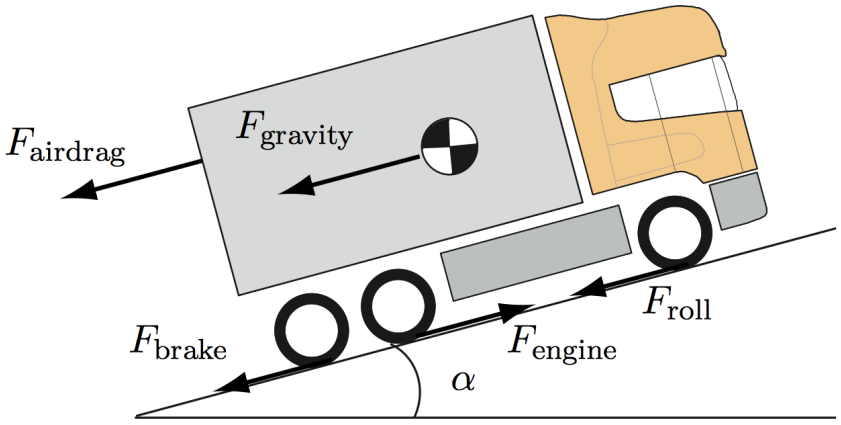

Figure 5.2: The longitudinal forces acting on a HDV in motion.

By applying Netwon's second law of motion:

$$m\dot{v} = F_w - F_{brake} - F_{airdrag} - F_{roll} - F_{gravity}$$

with eq. (5.10) the equation can be rewritten as:

$$m_t \dot{v} = F_{engine} - F_{brake} - F_{airdrag} - F_{roll} - F_{gravity} \tag{5.11}$$

where m denotes the vehicle mass and m_t is the accelerated mass given by:

$$m_t = m + \frac{J_w + i_t^2 i_f^2 \eta_t \eta_f J_e}{r_w^2}. \tag{5.12}$$

Aerodynamic force

The aerodynamic force is given by:

$$F_{airdrag}(v,d) = \frac{1}{2} c_D A_a \rho_a v^2 \tag{5.13}$$

where A_a is the maximal cross sectional area of the vehicle, and ρ_a is the air density. $c_D(d) = c_d(1 - \frac{f_i(d)}{100})$ is the air drag coefficient with the air drag reduction produced by the preceding vehicle. d is the intermediate distance between the vehicles and $f_i(d)$ is a non-linear function depicted in fig. 5.3 with i denoted as the ith vehicle in the platoon.

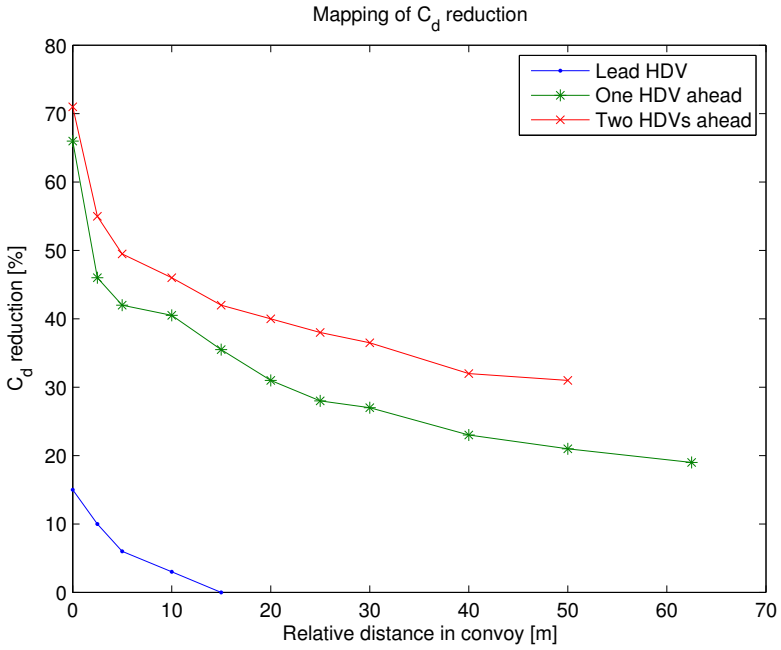

Figure 5.3: Empirical result of air drag reduction of HDV platooning (Alam et al., 2010).

Due to the non-linearity of $f_i(d)$, the function is approximated with a first order least square approximation giving the following:

$$\begin{aligned} f_1(d)_{ls} &= -0.9379d + 12.8966 \quad 0 \leq d \leq 15 \\ f_2(d)_{ls} &= -0.4502d + 43.0046 \quad 0 \leq d \leq 80 \\ f_3(d)_{ls} &= -0.4735d + 51.5027 \quad 0 \leq d \leq 80 \\ &\text{otherwise } f_i(d)_{ls} = 0 \end{aligned} \tag{5.14}$$

where $f_i(d)_{ls}$ is the least square approximation of the air drag reduction. It is assumed that the air drag reduction does not increase any further beyond the third vehicle.

Roll resistance

The roll resistance force is modeled as:

$$F_{roll}(\alpha) = c_r mg\cos(\alpha) \tag{5.15}$$

where c_r is the roll coefficient, and g is the gravitational constant.

Gravity

The gravitational force is given by:

$$F_{gravity}(\alpha) = mg\sin(\alpha). \tag{5.16}$$

Combined equations

By combining eqs. (5.10) to (5.16) together, a mathematical expression for the vehicle model can be expressed as:

$$\begin{aligned}\dot{v}_i = \frac{r_w^2}{J_w + mr_w^2 + i_t^2 i_f^2 \eta_t \eta_f J_e}\Bigg(&\frac{i_t i_f \eta_t \eta_f}{r_w} T_e - \frac{1}{2} c_d A_a \rho_a v^2 \\ &+ \frac{1}{2} c_d A_a \rho_a v^2 \frac{f_i(d)}{100} - c_r mg\cos(\alpha) - mg\sin(\alpha)\Bigg).\end{aligned} \tag{5.17}$$

By introducing the following five constants:

$$\begin{aligned}\kappa_1 &= \frac{r_w i_t i_f \eta_t \eta_f}{J_w + mr_w^2 + i_t^2 i_f^2 \eta_t \eta_f J_e} & \kappa_2 &= \frac{\frac{1}{2} r_w^2 A_a \rho_a c_d}{J_w + mr_w^2 + i_t^2 i_f^2 \eta_t \eta_f J_e} \\ \kappa_3 &= \frac{c_r r_w^2 mg}{J_w + mr_w^2 + i_t^2 i_f^2 \eta_t \eta_f J_e} & \kappa_4 &= \frac{r_w^2 mg}{J_w + mr_w^2 + i_t^2 i_f^2 \eta_t \eta_f J_e} \\ \phi_i(d) &= \left(1 - \frac{f_i(d)}{100}\right)\end{aligned} \tag{5.18}$$

the vehicle model from eq. (5.17) can be simplified to:

$$\dot{v}_i = \kappa_1 T_e - \kappa_2 \phi_i(d) v^2 - \kappa_3 \cos(\alpha) - \kappa_4 \sin(\alpha). \tag{5.19}$$

5.3 Linearized model

A linear quadratic solution will be utilized, therefore the non-linear model from eq. (5.17) needs to be linearized. The linearization point are chosen around a set reference velocity v_{ref}, a constant slope α_{ref}, a set distance d_{ref} and an engine torque that maintains the velocity. The equilibrium point are denoted by:

$$\begin{aligned}v_0 &= v_{ref} \\ \alpha_0 &= \alpha_{ref} \\ d_0 &= d_{ref} = \tau_{ref} v_0 \\ T_0 &= \frac{\kappa_2 \phi_i(d_0)_{ls} v_0^2 + \kappa_3 \cos(\alpha_0) + \kappa_4 \sin(\alpha_0)}{\kappa_1}.\end{aligned} \tag{5.20}$$

By applying a first order Taylor approximation around the equilibrium point in eq. (5.20), the following linearized model is obtained:

$$\begin{aligned}\dot{v}_i &\approx g'(v_0,\alpha_0,d_0,T_0) + g'_v(v_0,\alpha_0,d_0,T_0)\Delta v_i + g'_d(v_0,\alpha_0,d_0,T_0)\Delta d_i + g'_T(v_0,\alpha_0,d_0,T_0)\Delta T_i \\ &\approx -2\kappa_2\phi_i(d_0)_{ls}v_0\Delta v_i - \kappa_2\phi'_i(d_0)_{ls}v_0^2\Delta d_i + \kappa_1\Delta T_i \\ &= a_i\Delta v_i + b_i\Delta d_i + c_i\Delta T_i\end{aligned} \tag{5.21}$$

where:

$$\phi'_i(d)_{ls} = \frac{\mathrm{d}}{\mathrm{d}d}\left(1 - \frac{f_i(d)_{ls}}{100}\right) = \begin{cases} 0.009379 & i = 1 \\ 0.004502 & i = 2 \\ 0.004735 & i = 3. \end{cases}$$

The change in relative distance between two vehicles is described by:

$$\Delta\dot{d}_{i-1,i} = \Delta v_{i-1} - \Delta v_i. \tag{5.22}$$

The platoon model can now be written in a state-space equation through eqs. (5.21) and (5.22):

$$\begin{bmatrix} \Delta\dot{v}_1 \\ \Delta\dot{d}_{1,2} \\ \Delta\dot{v}_2 \\ \Delta\dot{d}_{2,3} \\ \Delta\dot{v}_3 \end{bmatrix} = \begin{bmatrix} a_1 & b_1 & 0 & 0 & 0 \\ 1 & 0 & -1 & 0 & 0 \\ 0 & b_2 & a_2 & 0 & 0 \\ 0 & 0 & 1 & 0 & -1 \\ 0 & 0 & 0 & b_3 & a_3 \end{bmatrix} \begin{bmatrix} \Delta v_1 \\ \Delta d_{1,2} \\ \Delta v_2 \\ \Delta d_{2,3} \\ \Delta v_3 \end{bmatrix} + \begin{bmatrix} c_1 & 0 & 0 \\ 0 & 0 & 0 \\ 0 & c_2 & 0 \\ 0 & 0 & 0 \\ 0 & 0 & c_3 \end{bmatrix} \begin{bmatrix} \Delta T_1 \\ \Delta T_2 \\ \Delta T_3 \end{bmatrix} \tag{5.23}$$

$$\Rightarrow \dot{x} = Ax + Bu.$$

Chapter 6

Optimal control

The optimal control theory is a mathematical optimization method to solve control theory problems. The problem to solve with optimal control is to find a control law for a given system with respect to given cost functions that is penalized if the states or inputs of the system get too large. If the dynamical system is described by linear equations and the costs is a quadratic function of the states and inputs, then the optimal control problem can be solved as a linear quadratic (LQ) problem.

The centralized controller for the platoon will be solved with two different LQ solutions. Firstly, a linear quadratic regulator (LQR) solution is used. This solution does not directly determine a reference signal that the vehicles can track, i.e. a velocity variation that can be followed. Therefore, to enable velocity tracking, the lead vehicle is equipped with the CC. The CC is set such that velocity changes can be done and the lead vehicle will follow the reference. This disables the property to control the lead vehicle with the LQR controller, hence only the two latter vehicles are controlled. The second centralized controller utilized is a linear quadratic tracking (LQT) with integral action. This solution allows a reference signal to be tracked. This enables a control law for the whole vehicle platoon, consisting of three vehicles.

The reason for two different LQ solutions is to achieve a better understanding of vehicle platooning. Is it better to let the lead vehicle drive with the CC and let the two following vehicles catch up or let the lead vehicle consider the vehicles behind and remain as a platoon? With that question in mind, the two control laws were obtained.

6.1 Linear Quadratic Regulator

The standard cost function setup for a LQR problem is shown in eq. (6.1):

$$J = \int_0^{t_f} \Big(x^T(\tau) Q x(\tau) + u^T(\tau) R u(\tau) \Big) \mathrm{d}\tau + x^T(t_f) Q_f x(t_f) \tag{6.1}$$

together with dynamic system constraints and initial conditions, the objective to minimize the cost function can be written as:

$$\begin{aligned} J^* = \min_u \int_0^{t_f} \Big(x^T(\tau)Qx(\tau) + u^T(\tau)Ru(\tau) \Big) \mathrm{d}\tau + x^T(t_f)Q_f x(t_f) \\ \text{Subject to: } \begin{cases} \dot{x}(t) &= Ax(t) + Bu(t) \\ x(0) &= x_0. \end{cases} \end{aligned} \tag{6.2}$$

This is called a finite horizon LQR and requires information ahead of time, such as the look-ahead. In order to solve the LQR problem, three requirements need to be satisfied. The pair (A, B) needs to be controllable, the cost matrices Q and Q_f need to be positive semi definite, and R needs to be positive definite.

The platoon model described in chapter 5 is linearized around an equilibrium point. Therefore, this LQR setup penalizes when the states or inputs deviate from the equilibrium point. By minimizing the input, i.e. the torque, the fuel will also be minimized by the relation shown in eq. (5.2). For a detailed explanation of the LQR derivation, the reader is referred to read appendix B.

A solution for a finite horizon LQR is to apply dynamic programming (DP). First set $P(t_f) = Q_f$ and work from time t_f and backward to the initial time, zero. This is done by solving the Riccati differential equation, numerically:

$$-\dot{P}(t) = A^T P(t) + P(t)A^T - P(t)BR^{-1}B^T P(t) + Q. \tag{6.3}$$

At time t, the optimal control u_{opt} is given by:

$$u_{opt}(t) = K(t)x(t) \tag{6.4}$$

where

$$K(t) = -R^{-1}B^T P(t).$$

Repeat the steps and work the way back for all $t \in [0, t_f]$ for an optimal control over all t. This DP method extends to time-varying A, B, Q and R matrices.

A more simple case is when the matrices A, B, Q and R are constant together with an infinite horizon problem. The cost function and conditions is then given by:

$$\begin{aligned} J^* = \min_u \int_0^{\infty} x^T(\tau)Qx(\tau) + u^T(\tau)Ru(\tau)\, \mathrm{d}\tau \\ \text{Subject to: } \begin{cases} \dot{x}(t) &= Ax(t) + Bu(t) \\ x(0) &= x_0. \end{cases} \end{aligned} \tag{6.5}$$

This system requires no preview information and is considered to be in steady state. Therefore, the Riccati differential equation, eq. (6.3), can now be considered as an Algebraic Riccati Equation (ARE):

$$A^T P_{ss} + P_{ss}A^T - P_{ss}BR^{-1}B^T P_{ss} + Q = 0. \tag{6.6}$$

Equation (6.6) needs to be solved numerically and with the numerical solution, the optimal control u_{opt} is given by:

$$u_{opt}(t) = -R^{-1}B^T P_{ss} x(t). \tag{6.7}$$

6.2 Linear Quadratic Tracking control with integral action

The idea of this solution is to let the lead vehicle follow a reference signal, in this case a velocity reference. This allows the lead vehicle to track a set reference velocity smoothly with a LQ solution. Since it is a centralized control, the lead vehicle will also take the following vehicles into account, which the LQR solution lacks. The following method follows the same derivation as in (Groves et al., 2005).

6.2.1 Reference tracking system

The concept is to introduce an error: $\dot{e} = r - x$, where r is one or several reference signals. By including an integrating action, the feedback control eliminates the steady state error of the system. Hence, the integral error is given by $e = \int \dot{e}\,\mathrm{d}t$, which is introduced as a new state to the dynamic system:

$$\begin{bmatrix} \dot{e} \\ \dot{x} \end{bmatrix} = \begin{bmatrix} 0 & -I \\ 0 & A \end{bmatrix} \begin{bmatrix} e \\ x \end{bmatrix} + \begin{bmatrix} 0 \\ B \end{bmatrix} u + \begin{bmatrix} I \\ 0 \end{bmatrix} r \tag{6.8}$$

$$\Rightarrow \dot{\tilde{x}} = \tilde{A}\tilde{x} + \tilde{B}u + Gr.$$

The error system for eq. (6.8) can then be defined as:

$$\tilde{e} = \begin{bmatrix} e \\ r - x \end{bmatrix} = Mr + H\tilde{x} \tag{6.9}$$

where:

$$M = \begin{bmatrix} 0 \\ I \end{bmatrix} \quad H = \begin{bmatrix} I & 0 \\ 0 & -I \end{bmatrix}.$$

This will serve as a premise for the LQT cost function in section 6.2.3.

6.2.2 Reference tracking platoon model

By adapting the platoon model, eq. (5.23), with the reference tracking system described in section 6.2.1, the new dynamical system can be described as:

$$\begin{aligned}\begin{bmatrix} \Delta\dot{e} \\ \Delta\dot{v}_1 \\ \Delta\dot{d}_{1,2} \\ \Delta\dot{v}_2 \\ \Delta\dot{d}_{2,3} \\ \Delta\dot{v}_3 \end{bmatrix} &= \begin{bmatrix} 0 & -1 & 0 & 0 & 0 & 0 \\ 0 & a_1 & b_1 & 0 & 0 & 0 \\ 0 & 1 & 0 & -1 & 0 & 0 \\ 0 & 0 & b_2 & a_2 & 0 & 0 \\ 0 & 0 & 0 & 1 & 0 & -1 \\ 0 & 0 & 0 & 0 & b_3 & a_3 \end{bmatrix} \begin{bmatrix} \Delta e \\ \Delta v_1 \\ \Delta d_{1,2} \\ \Delta v_2 \\ \Delta d_{2,3} \\ \Delta v_3 \end{bmatrix} + \\ &+ \begin{bmatrix} 0 & 0 & 0 \\ c_1 & 0 & 0 \\ 0 & 0 & 0 \\ 0 & c_2 & 0 \\ 0 & 0 & 0 \\ 0 & 0 & c_3 \end{bmatrix} \begin{bmatrix} \Delta T_1 \\ \Delta T_2 \\ \Delta T_3 \end{bmatrix} + \begin{bmatrix} 1 \\ 0 \\ 0 \\ 0 \\ 0 \\ 0 \end{bmatrix} r \end{aligned} \tag{6.10}$$

$$\Rightarrow \dot{\tilde{x}} = \tilde{A}\tilde{x} + \tilde{B}u + Gr$$

where $\Delta e = \int (r - \Delta v_1)$.

The new error system is defined as:

$$\tilde{e} = \begin{bmatrix} \Delta e \\ r - \Delta v_1 \\ \Delta d_{1,2} \\ \Delta v_2 \\ \Delta d_{2,3} \\ \Delta v_3 \end{bmatrix} = \begin{bmatrix} 0 \\ 1 \\ 0 \\ 0 \\ 0 \\ 0 \end{bmatrix} r + \begin{bmatrix} 1 & 0 & 0 & 0 & 0 & 0 \\ 0 & -1 & 0 & 0 & 0 & 0 \\ 0 & 0 & 1 & 0 & 0 & 0 \\ 0 & 0 & 0 & 1 & 0 & 0 \\ 0 & 0 & 0 & 0 & 1 & 0 \\ 0 & 0 & 0 & 0 & 0 & 1 \end{bmatrix} \begin{bmatrix} \Delta e \\ \Delta v_1 \\ \Delta d_{1,2} \\ \Delta v_2 \\ \Delta d_{2,3} \\ \Delta v_3 \end{bmatrix} \tag{6.11}$$

$$\Rightarrow \tilde{e} = Mr + H\tilde{x}.$$

6.2.3 LQ optimal control

The cost function for a LQ problem with finite horizon now follows as:

$$\begin{aligned} J &= \int_0^{t_f} \left(\tilde{e}^T(\tau) Q \tilde{e}(\tau) + u^T(\tau) R u(\tau) \right) \mathrm{d}\tau + \tilde{e}^T(t_f) Q_f \tilde{e}(t_f) \\ \text{Subject to: } &\begin{cases} \dot{\tilde{e}}(t) &= H\tilde{A}\tilde{x}(t) + H\tilde{B}u(t) + HGr(t) \\ \tilde{e}(0) &= \tilde{e}_0 \end{cases} \end{aligned} \tag{6.12}$$

with the assumption that $\dot{r} = 0$ and by inserting eq. (6.9), the expanded cost function is:

$$\begin{aligned} J = &\int_0^{t_f} \left(\tilde{x}^T H^T Q H \tilde{x} + 2r^T M^T Q H \tilde{x} + r^T M^T Q M r + u^T R u\right) \mathrm{d}\tau + \\ &+\tilde{x}^T(t_f) H^T Q_f H \tilde{x}(t_f) + 2r^T(t_f) M^T Q_f H \tilde{x}(t_f) + r^T(t_f) M^T Q_f M r(t_f) \\ &\text{Subject to: } \begin{cases} \dot{\tilde{x}}(t) &= \tilde{A}\tilde{x}(t) + \tilde{B}u(t) + Gr(t) \\ \tilde{x}(0) &= \tilde{x}_0. \end{cases} \end{aligned} \tag{6.13}$$

The requirement remains the same as for the LQR case. The pair $(\tilde{A}, \tilde{B})$ must be controllable, and the cost matrices Q and Q_f are positive semi definite while R is positive definite. This gives the following differential equations (readers are referred to appendix C for the derivation):

$$\dot{P} = -P\tilde{A} - \tilde{A}^T P - H^T Q H + P\tilde{B}R^{-1}\tilde{B}^T P \tag{6.14a}$$

$$\dot{g} = \left(P\tilde{B}R^{-1}\tilde{B}^T - \tilde{A}^T\right) g - \left(H^T Q M + PG\right). \tag{6.14b}$$

Equation (6.14a) is the same standard Riccati equation as eq. (6.3), while eq. (6.14b) is an auxiliary vector equation that defines the feedforward gain.

By assuming constant $\tilde{A}, \tilde{B}, Q$ and R with infinite horizon, the controller can be assumed to be in steady state, i.e. $\dot{P} = 0$ and $\dot{g} = 0$. The following optimal control u_{opt} is obtained as:

$$u_{opt}(t) = K_x \tilde{x}(t) + K_r r(t) \tag{6.15}$$

where:

$$\begin{aligned} K_x &= -R^{-1}\tilde{B}^T P_{ss} \\ K_r &= -R^{-1}\tilde{B}^T \left(P_{ss}\tilde{B}R^{-1}\tilde{B}^T - \tilde{A}^T\right)^{-1} \left(H^T Q M + P_{ss} G\right). \end{aligned}$$

6.3 Cost function design

Normally, the difficult part with utilizing a LQ solution is the choice of cost matrices, in this case Q and R. The matrices determine how the dynamical system performs and should therefore be chosen such that the desired performance is achieved. The costs and cost matrices will vary for the two LQ solutions, due the additional states i.e. the reference signal and the accumulated error. However, a general idea for the vehicle platoon, from eq. (5.23), is described.

It is important that the vehicles in a platoon do not collide within the platoon, hence the vehicle should not deviate from the set time gap. Therefore, the difference between the relative distance and set distance gap should be penalized:

$$d_{i-1,i} - \tau v_i = (\Delta d_{i-1,i} + d_{ref}) - \tau(\Delta v_i + v_{ref}) = \Delta d_{i-1,i} - \tau \Delta v_i.$$

The vehicle performance can be smoother by also adjusting the velocity according to the velocity of the vehicle ahead, hence:

$$v_{i-1} - v_i = (\Delta v_{i-1} + v_{ref}) - (\Delta v_i + v_{ref}) = \Delta v_{i-1} - \Delta v_i.$$

Lastly, the torque inputs should be penalized from its equilibrium point to maintain a low fuel consumption:

$$\Delta T_i.$$

The LQR cost function can now be described as:

$$\begin{aligned} J = \int_0^\infty \Big(\varphi_1^d (\Delta d_{1,2} - \tau \Delta v_2)^2 + \varphi_2^d (\Delta d_{2,3} - \tau \Delta v_3)^2 + \varphi_1^v (\Delta v_1 - \Delta v_2)^2 + \\ + \varphi_2^v (\Delta v_2 - \Delta v_3)^2 + \varphi_1^T \Delta T_2^2 + \varphi_2^T \Delta T_3^2 \Big) \, \mathrm{d}\tau. \end{aligned} \tag{6.16}$$

Notice that ΔT_1 is not penalized in the LQR solution, which was mentioned in the introduction of chapter 6. The lead vehicle utilizes the CC to maintain its own speed without regarding the following vehicles. The cost function for the LQT is slightly different, with additional penalties for torque input for the lead vehicle, the accumulating error, the reference deviation $r - \Delta v_1$, and relative distance between vehicle 1 and 3.

Equation (6.16) can now be written in matrix form where the cost matrices are as follows:

$$Q_{LQR} = \begin{bmatrix} \varphi_1^v & 0 & -\varphi_1^v & 0 & 0 \\ 0 & \varphi_1^d & -\tau\varphi_1^d & 0 & 0 \\ -\varphi_1^v & -\tau\varphi_1^d & \varphi_1^v + \tau^2\varphi_1^d + \varphi_2^v & 0 & -\varphi_2^v \\ 0 & 0 & 0 & \varphi_2^d & -\tau\varphi_2^d \\ 0 & 0 & -\varphi_2^v & -\tau\varphi_2^d & \varphi_2^v + \tau^2\varphi_2^d \end{bmatrix} \tag{6.17}$$

$$R_{LQR} = \begin{bmatrix} \varphi_1^T & 0 \\ 0 & \varphi_2^T \end{bmatrix}.$$

Similar method gives the cost matrices for the LQT solution:

$$Q_{LQT} = \begin{bmatrix} \varphi^e & 0 & 0 & 0 & 0 & 0 \\ 0 & \varphi_1^v & 0 & 0 & 0 & 0 \\ 0 & 0 & \varphi_1^d + \varphi_3^d & -\tau(\varphi_1^d + \varphi_3^d) & \varphi_3^d & -\tau\varphi_3^d \\ 0 & 0 & -\tau(\varphi_1^d + \varphi_3^d) & \tau^2(\varphi_1^d + \varphi_3^d) + \varphi_2^v & -\tau\varphi_3^d & -\varphi_2^v + \tau^2\varphi_3^d \\ 0 & 0 & \varphi_3^d & -\tau\varphi_3^d & \varphi_2^d + \varphi_3^d & -\tau(\varphi_2^d + \varphi_3^d) \\ 0 & 0 & -\tau\varphi_3^d & -\varphi_2^v + \tau^2\varphi_3^d & -\tau(\varphi_2^d + \varphi_3^d) & \varphi_2^v + \tau^2(\varphi_2^d + \varphi_3^d) \end{bmatrix}$$

$$R_{LQT} = \begin{bmatrix} \varphi_1^T & 0 & 0 \\ 0 & \varphi_2^T & 0 \\ 0 & 0 & \varphi_3^T \end{bmatrix}. \tag{6.18}$$

Chapter 7

Simulation

The simulations were done in Simulink with a vehicle model made by Scania CV AB. A few modifications were made to enable platooning and the implementation of the proposed controllers. To analyze the effect a platoon has on fuel consumption, a few fuel saving functionalities such as downhill speed control and look-ahead were removed. This is to obtain more accurate simulation results, and also due to the reason that the proposed controllers cannot take those features into account. The obtained Simulink model did not have a fuel consumption output, however the consumed energy in the engine was obtainable. The consumed energy is almost proportional to the fuel consumption, and is therefore a valid result to analyze.

7.1 Simulation scenario

A scenario with velocity changes were simulated on a 4.5 km long flat road. The three vehicles are identical and the weight is set to 40 tonnes each. The scenario starts with the platoon driving at 80 km/h, thereafter brake to 70 km/h at $t = 50$ s. After holding the speed for 50 s, the platoon accelerates to 85 km/h and lastly, at $t = 150$ s, a short deceleration back to 80 km/h occurs before reaching the goal. The reason for the small velocity changes is that the linearized model with a LQ solution cannot guarantee optimal performance for large deviations from the equilibrium point. The set scenario is to examine if the LQ controllers can manage sudden velocity changes such that the vehicles in the platoon do not collide. Different time headways are used to analyze the saved energy potentials compared to the safety aspects. The time headways used are τ: 0.25, 0.5, 0.75, and 1 s. The reference result that both LQ controllers will be compared to, is a single vehicle with CC on the same road profile.

7.2 Different time headways

Different time headways are used in order to compare the energy saved with the relative distance. A closer distance is more sensitive to time delays and package

losses, due to the short time headway for any possible maneuvers. The result from (Alam et al., 2011) indicates a minimum relative distance of 1.2 m between two identical HDVs can be obtained without endangering a collision. This is assumed with no delays in the system and that the HDV can achieve maximum brake capacity instantaneously. A brief calculation of a time delay of 500 ms shows that the intermediate distance only has to be increased to 2 m to avoid collision. Although this project does not consider any disturbances, the risks must be considered for real life appliciation

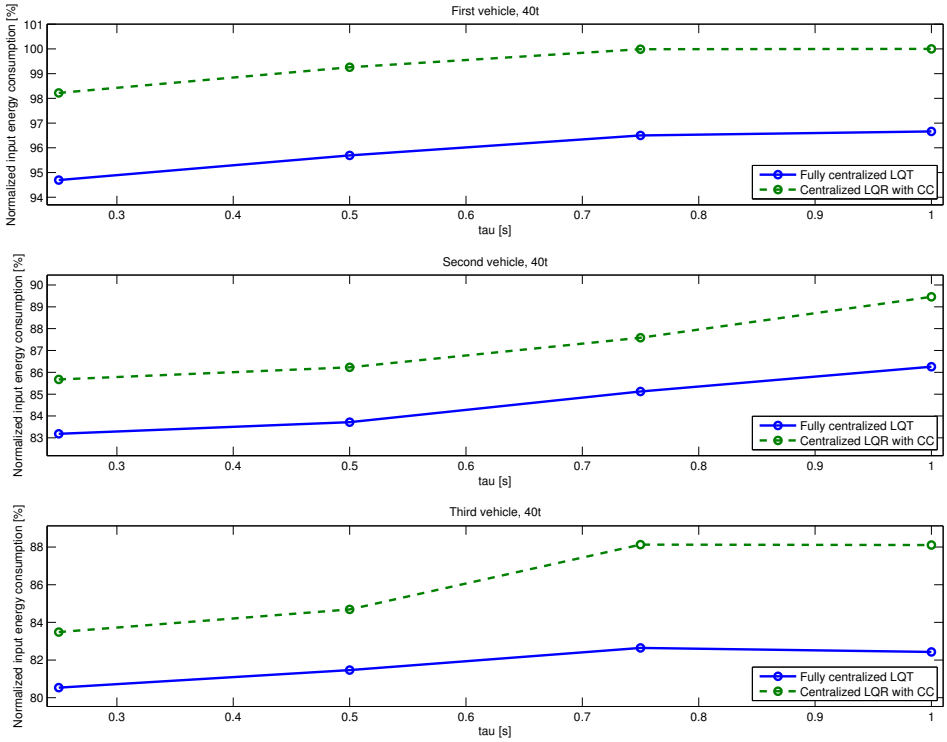

Figure 7.1: Energy saved for each vehicle separately compared to a single vehicle with the CC driving on a flat road with vehicle changes.

Figures 7.1 and 7.2 show the results from the simulations utilizing two different LQ controls, normalized against a single vehicle driving with the CC on the same road profile. Figure 7.1 shows the consumed energy for each vehicle in the platoon. It can be seen that the first vehicle with the LQR only reduces a small amount of the energy when the following vehicle is relatively close. In this case, only when the time headway is set to $\tau \leq 0.75$ s, thus allowing the following vehicle be close enough to enable a small air drag reduction for the lead vehicle. The saving potentials are vast for the second and third vehicle for all simulated time headways. Figure 7.2 shows the results as a whole platoon compared to a single vehicle using the CC, by comparing consumed energy, time difference, and average velocity. The time

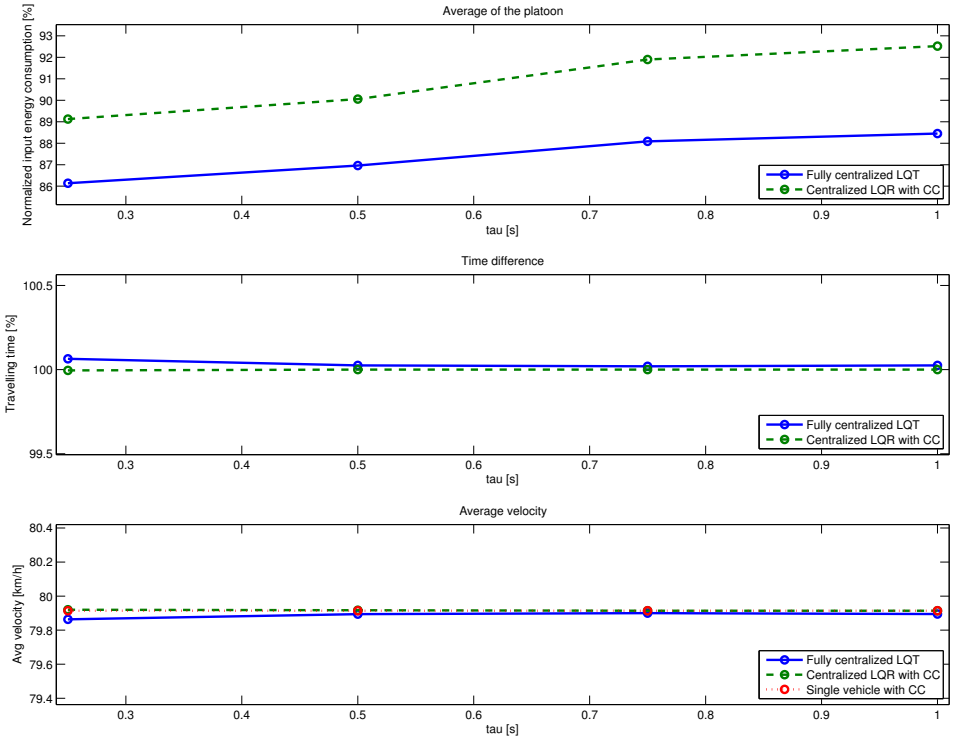

Figure 7.2: The average consumed energy, time, and velocity differences compared to a single vehicle with the CC driving on a flat road with velocity changes.

Table 7.1: Summary of figs. 7.1 and 7.2, comparing different controllers with a single vehicle with the CC on a flat road with velocity changes.

	LQR control				**LQT control**			
Tau, τ	**0.25 s**	**0.5 s**	**0.75 s**	**1 s**	**0.25 s**	**0.5 s**	**0.75 s**	**1 s**
Avg velocity [km/h]	79.92	79.92	79.91	79.91	79.86	79.89	79.90	79.89
Time saved [%]	0.00	0.00	0.00	0.00	-0.06	-0.02	-0.02	-0.02
Vehicle 1 energy saved [%]	1.78	0.74	0.01	0.00	5.31	4.31	3.50	3.34
Vehicle 2 energy saved [%]	14.33	13.77	12.42	10.54	16.82	16.32	14.88	13.74
Vehicle 3 energy saved [%]	16.52	15.31	11.87	11.89	19.46	18.53	17.36	17.57
Avg energy saved [%]	10.87	9.94	8.10	7.48	13.86	13.04	11.91	11.55

and average velocity do not differ noticeably, however the obtained energy saving potentials are large.

Table 7.1 summarizes both the results from figs. 7.1 and 7.2. The analysis shows that the LQT controller is more energy efficient for all vehicles with barely any time or velocity differences. The main reason lies in the cruise control, it is not optimized to be an energy efficient function. The CC only maintains the set vehicle velocity and has a slight overshooting behavior, which cannot be considered energy efficient. The LQR control does not control the first vehicle, which uses the CC to maintain a velocity. The following vehicles are imitating the behavior of the lead vehicle, hence the whole platoon suffers the same loss from the CC behavior.

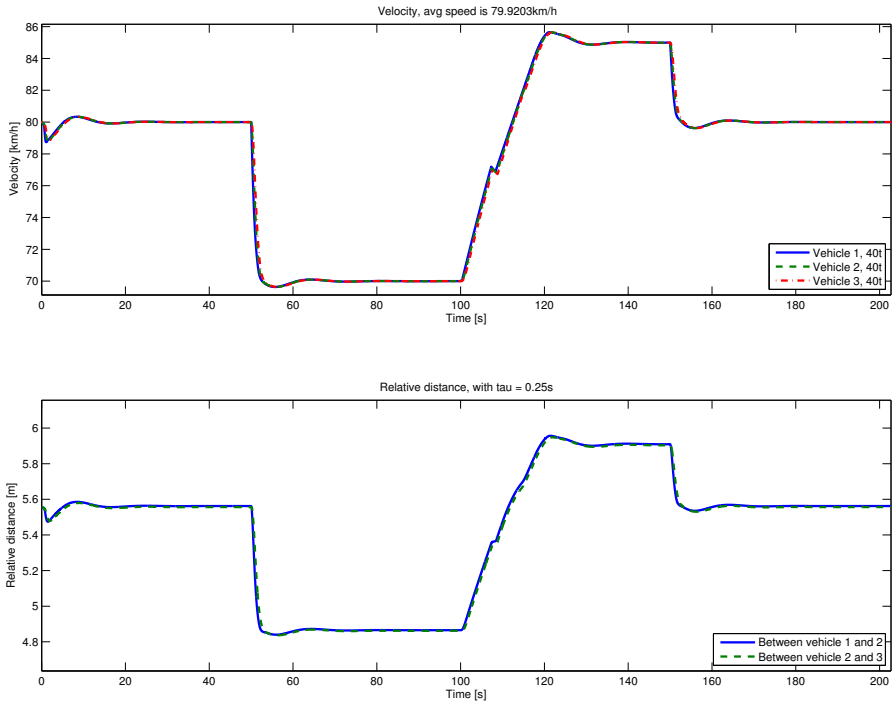

Figure 7.3: Three-vehicle platoon utilizing LQR control with CC on a flat road, with time headway $\tau = 0.25\,\mathrm{s}$. The velocity and relative distance are plotted.

The performance and behavior of the platoon are also important to analyze. The velocity and relative distance profile utilizing the LQR control on a flat road are depicted in fig. 7.3. Figure 7.4 illustrates the similar, however with the LQT control. Both controllers display a relatively good following behavior where the platoon hardly deviates from the set time headway, in this case $\tau = 0.25\,\mathrm{s}$. As earlier mentioned, the CC is not optimized to be an energy efficient function and this can be seen in fig. 7.3, where it produces an overshoot during brake and acceleration. This can be compared to fig. 7.4 where the tracking control is utilized, it has smooth

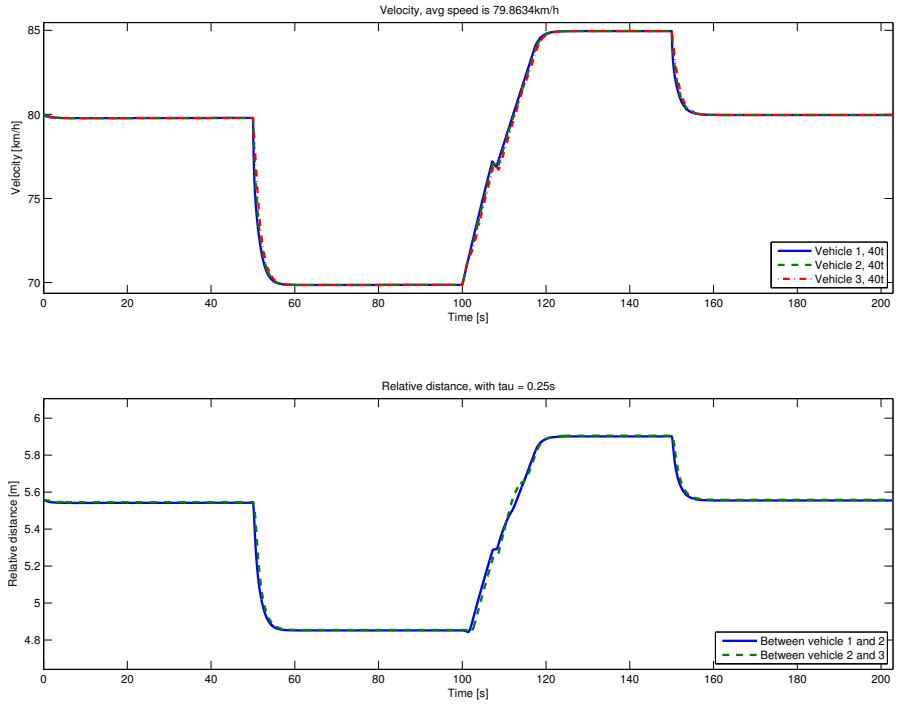

Figure 7.4: Three-vehicle platoon utilizing LQT control on a flat road, with time headway $\tau = 0.25\,\mathrm{s}$. The velocity and relative distance are plotted.

transitions between the velocity changes without any overshoots. The drawback with the smooth transition is the slightly lower deceleration when braking.

The notch at $t = 108\,\mathrm{s}$ in figs. 7.3 and 7.4 represents the vehicle gear shifting. Although the gear shifting does not seem to cause issues for the two displayed figures, it can actually have an impact on the platooning behavior. Figure 7.5 illustrates the same road profile with the LQR controller, however the time headway is increased to $\tau = 1\,\mathrm{s}$. This clearly shows that gear shifting is delayed for the following vehicles, which in turn causes a wider intermediate distance. The following vehicles are therefore accelerating longer in order to compensate for the distance loss. However, a platoon with the LQT control responds differently, which is depicted in fig. 7.6. Instead of having the following vehicles drive in a higher velocity, the lead vehicle accelerates slower in order to compensate for the increased distance gap. This can be noticed in the saved energy for the third vehicle in table 7.1, where the saving potential is dropped by a lot with a higher time headway. This ultimately shows the main difference between considering and not considering the following vehicles in a platoon. With information from the following vehicles and vehicles ahead allows the platoon to act more as one unit.

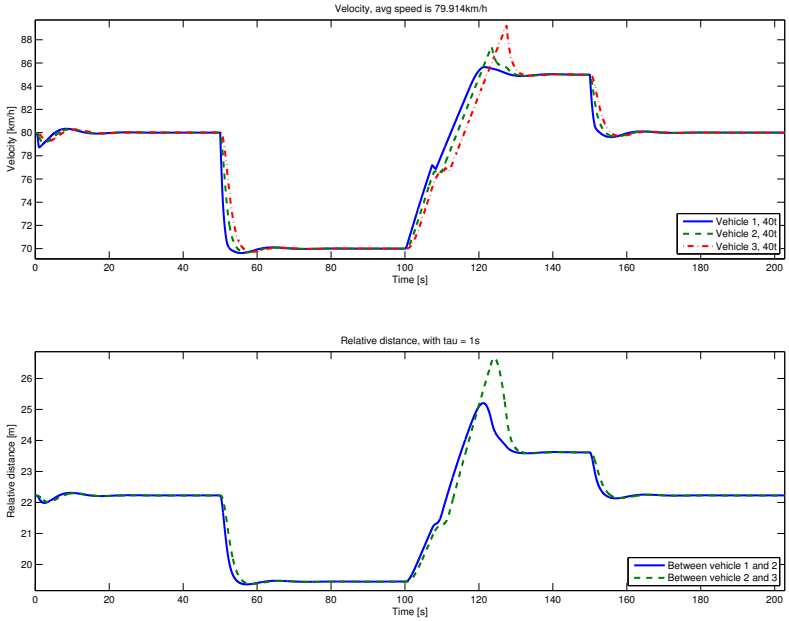

Figure 7.5: Three-vehicle platoon utilizing LQR control with CC on a flat road, with time headway $\tau = 1\,\mathrm{s}$. The velocity and relative distance are plotted.

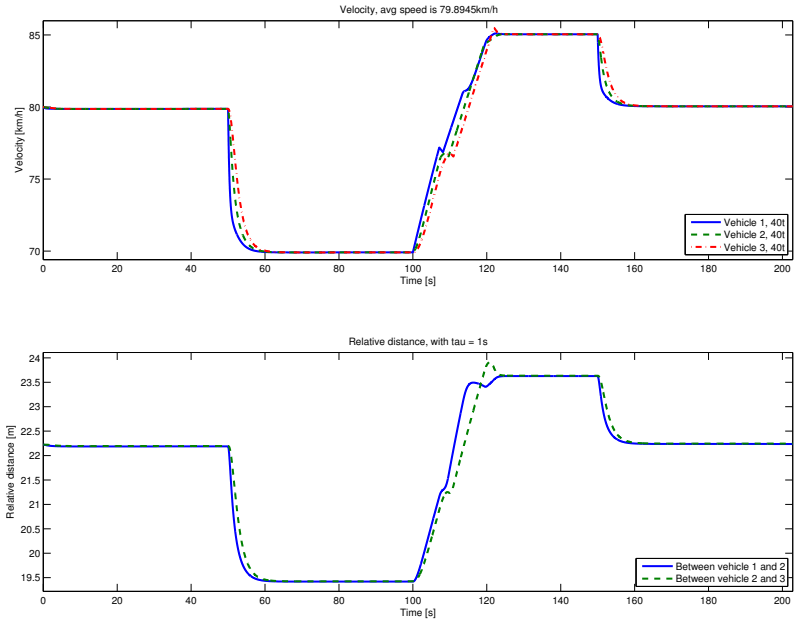

Figure 7.6: Three-vehicle platoon utilizing LQT control on a flat road, with time headway $\tau = 1\,\mathrm{s}$. The velocity and relative distance are plotted.

7.3 Change in mass distribution

Different vehicle weights have different dynamics, therefore, it is necessary to analyze the platoon behavior with mass variations. Although this is more difficult to analyze numerically, it is instead simulated with two different weights on the second vehicle in the platoon. Simulations of a lighter middle HDV with the weight of 30 tonnes and a heavier HDV with 50 tonnes are done.

7.3.1 40-30-40 tonnes platoon

A platoon, consisting of a 40 tonnes lead vehicle followed by a 30 tonnes HDV and lastly a 40 tonnes HDV as the tail vehicle, is simulated with both the LQ controllers. The time headway is set to $\tau = 0.25\,\mathrm{s}$. This is done to analyze how mass differences in the platoon affect the platoon behavior.

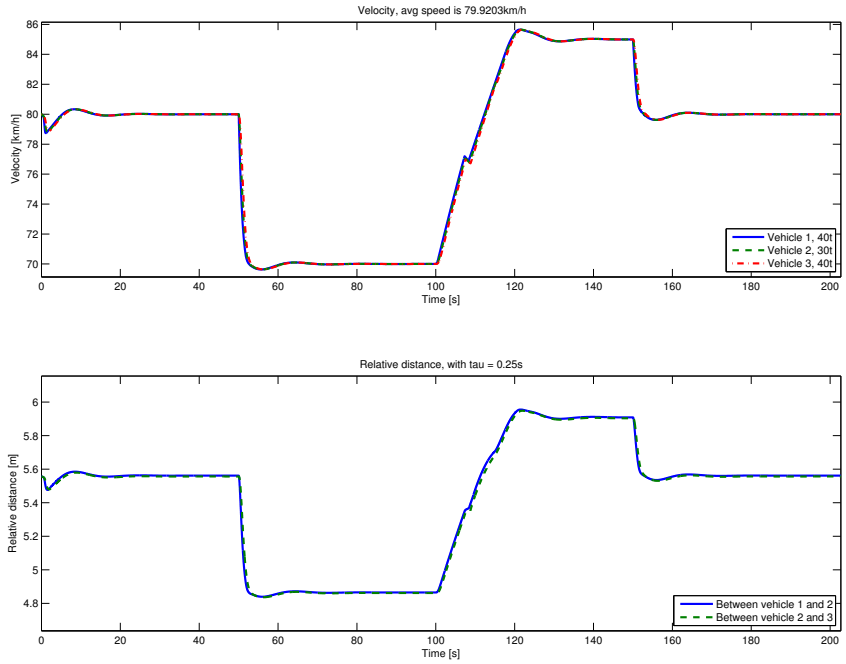

Figure 7.7: A 40-30-40 tonnes platoon with LQR control traveling on a flat road. The velocity and relative distance are plotted.

Figures 7.7 and 7.8 illustrate the velocity and relative distance behaviors for both LQ controllers. The figures do not show any irregular behavior, which was expected. A lighter vehicle with the same truck properties as a 40 tonnes HDV should not have problems maintaining the velocity and the intermediate distance.

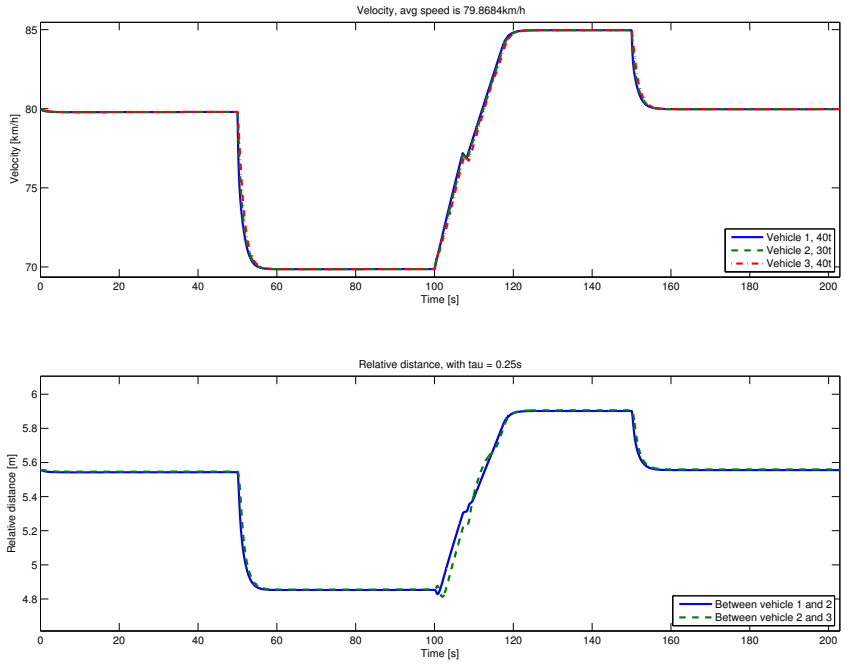

Figure 7.8: A 40-30-40 tonnes platoon with LQT control traveling on a flat road. The velocity and relative distance are plotted.

7.3.2 40-50-40 tonnes platoon

The mass of the second vehicle of the platoon has now been increased to 50 tonnes, and the time headway still remains at $\tau = 0.25\,\mathrm{s}$. A heavier HDV in the middle of the platoon should establish velocity issues, unless the engine is powerful enough to maintain the same velocity as the preceding vehicle.

The simulation results are depicted in fig. 7.9 for the LQR control and fig. 7.10 for the LQT control. The heavier HDV cannot keep up with the lighter HDV in front during acceleration, and therefore the distance gap widens. To compensate the distance loss, the heavier HDV accelerates longer to obtain a higher velocity. In this case, a velocity over the allowed limit for HDVs in Sweden, i.e. $90\,\mathrm{km/h}$. The LQ control cannot take the speed limit into account, and is therefore possible for the vehicle to accelerate past the speed limit. A solution to solve this issue is to have a parallel controller calculating what speed the HDV obtains. If the HDV is past the speed limit, the parallel controller would then cut off the torque input, but this is not taken into account in this project. However, the platoon with the LQT controller acts differently. The first vehicle accelerates slower, as in section 7.2, which can be noted in the additional notch in the velocity in fig. 7.10.

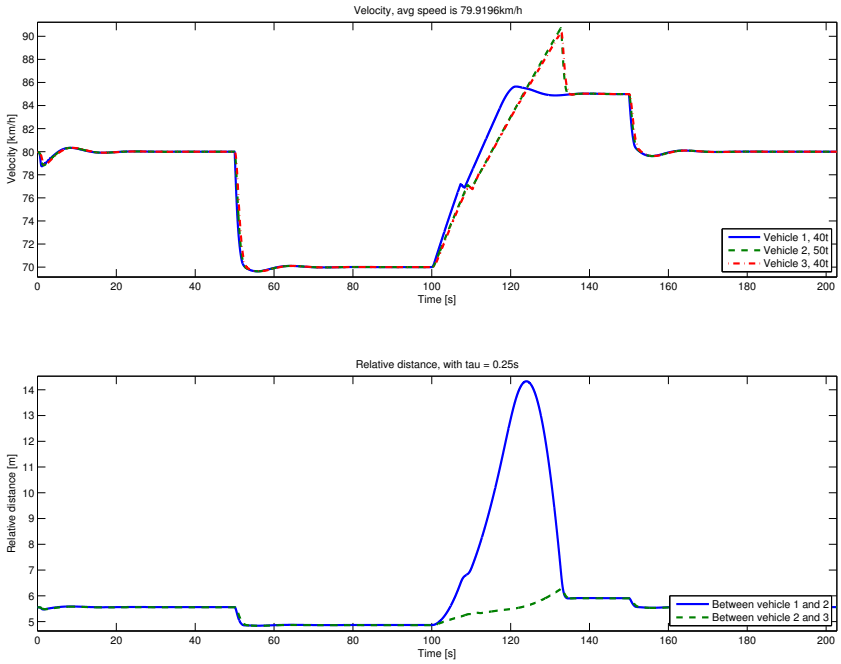

Figure 7.9: A 40-50-40 tonnes platoon with LQR control traveling on a flat road. The velocity and relative distance are plotted.

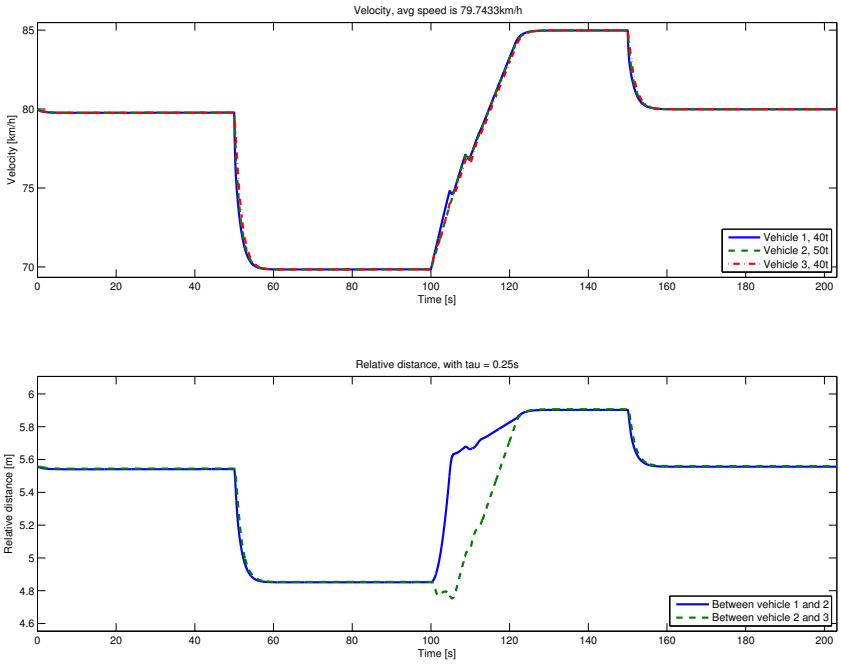

Figure 7.10: A 40-50-40 tonnes platoon with LQT control traveling on a flat road. The velocity and relative distance are plotted.

7.4 Simulation on a measured road profile

There are rarely any long flat roads in Sweden. Therefore, simulations on a real road profile is done to see how the topography affects the platoon behavior. The highway from Södertälje to Norrköping is approximately 120 km long, which will be used in the simulation. Identical HDVs are used, with a mass of 40 tonnes each.

7.4.1 Södertälje to Norrköping

Figures 7.11 and 7.12 show the results of consumed energy and average velocity against the set time headway for both LQ controllers. The benchmark is a single HDV driving the same road with the CC. Table 7.2 summarizes the results from both figures.

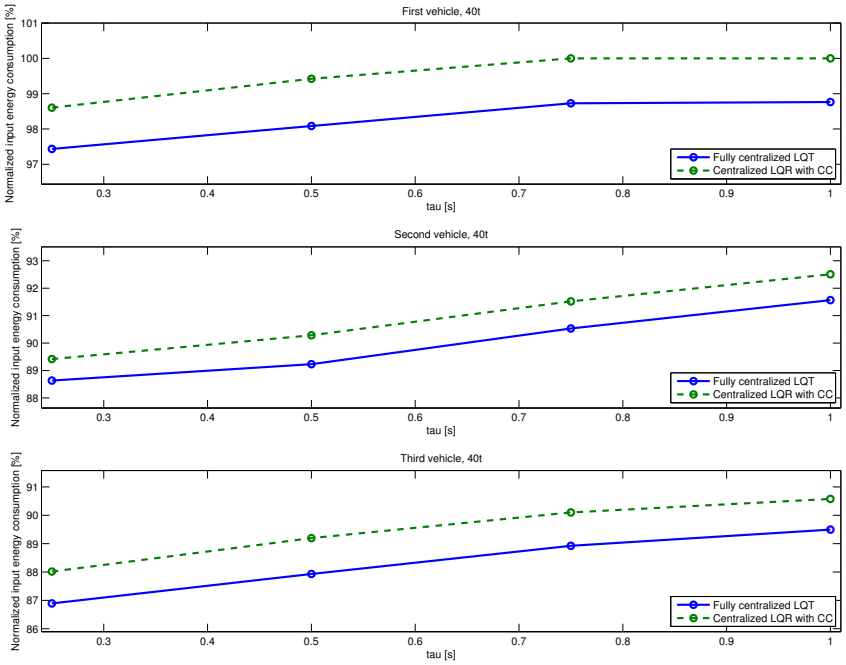

Figure 7.11: Energy saved for each vehicle separately compared to a single vehicle with CC driving on the highway from Södertälje to Norrköping.

The energy reduction for each vehicle is large, but not as large as with the previous simulations on a flat road. The gap of saving potentials between the LQR and LQT control has decreased. The LQT control is still more energy efficient, with approximately 1 percentage per vehicle compared to 3 percentage on the flat road. The explanation is due to the frequent topography change, which causes overshooting behaviors for both controls. Since the LQR control is already overshooting during velocity change, the topography variations may not cause a large impact as

on the LQT control. Otherwise, both platoons present good vehicle following behavior when the platoon consists of identical vehicles, indicated in figs. 7.13 and 7.14.

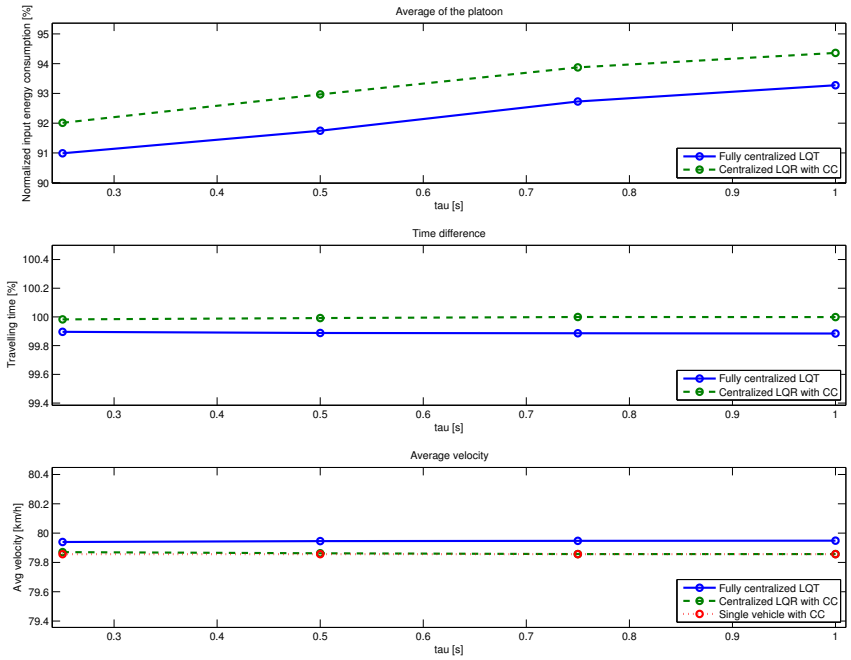

Figure 7.12: The average consumed energy, time, and velocity differences compared to a single vehicle with CC driving on the highway from Södertälje to Norrköping.

Table 7.2: Summary of figs. 7.11 and 7.12, comparing different controllers with a single vehicle with CC on the highway from Södertälje to Norrköping

	LQR control				**LQT control**			
Tau, τ	**0.25 s**	**0.5 s**	**0.75 s**	**1 s**	**0.25 s**	**0.5 s**	**0.75 s**	**1 s**
Avg velocity [km/h]	79.86	79.86	79.86	79.86	79.94	79.95	79.95	79.95
Time saved [%]	0.00	0.00	0.00	0.00	0.10	0.11	0.11	0.12
Vehicle 1 energy saved [%]	1.40	0.58	-0.00	-0.00	2.56	1.92	1.27	1.24
Vehicle 2 energy saved [%]	10.58	9.72	8.48	7.49	11.37	10.77	9.47	8.43
Vehicle 3 energy saved [%]	11.99	10.80	9.90	9.42	13.11	12.07	11.08	10.51
Avg energy saved [%]	7.99	7.03	6.13	5.64	9.01	8.25	7.27	6.73

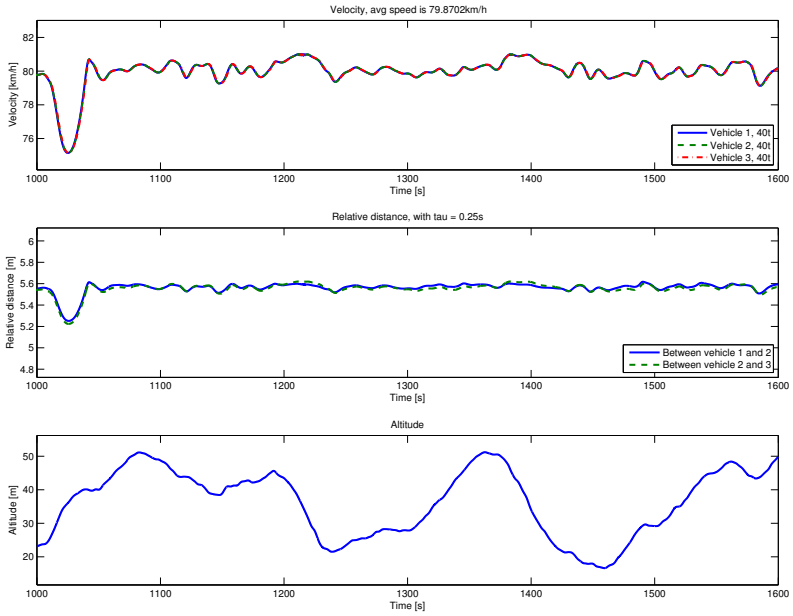

Figure 7.13: A part of the highway between Södertälje and Norrköping. The platoon utilizes the LQR control with CC. The velocity, relative distance and altitude is plotted.

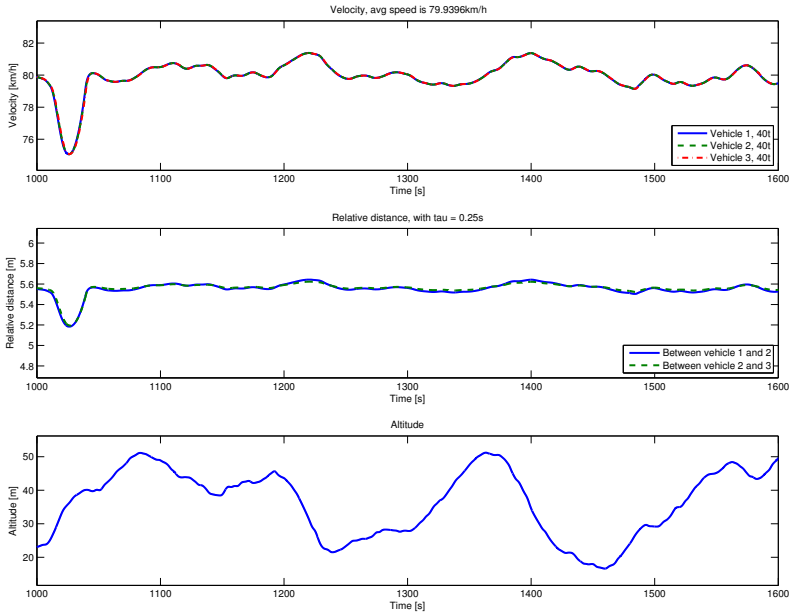

Figure 7.14: A part of the highway between Södertälje and Norrköping. The platoon utlizes the LQT control. The velocity, relative distance and altitude is plotted.

Chapter 8

Expanding the platoon

8.1 Sub-platoons within the platoon

It is desirable to have a longer platoon consisting of more than three vehicles. Therefore, a method is introduced to expand the centralized three-vehicle platoon to a longer platoon consisting of several sub-platoons. The solution is to utilize the both proposed controllers with a switcher between the LQR and the LQT control. To avoid a rash following behavior after a gear shift from the LQR control, mentioned at the end of section 7.2, a transition phase is introduced when switching between the controllers. This will also limit the velocity of the following sub-platoon to the set velocity reference.

The idea is illustrated in fig. 8.1. The sub-platoons utilize the LQT control when it is far from the sub-platoon ahead, thus traveling independently. When another sub-platoon is within range, it changes to a transition phase where the following sub-platoon slowly decreases the velocity and adapting the velocity to the sub-platoon ahead. This is done by ramping down the velocity reference signal of the LQT control. Lastly, when the sub-platoon is close enough, it switches to the LQR control and follows the tail vehicle of the sub-platoon ahead. This allows arbitrary long platoons, where the platoon is decentralized but consists of centralized sub-platoons.

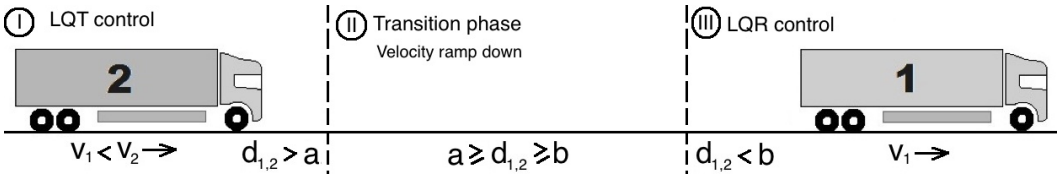

Figure 8.1: The general idea of a transition phase between the switchings of two LQ controls.

8.2 Simulation verification

To verify the switching control, a simple simulation on a flat road is done. The lead sub-platoon starts at 70 km/h and is 300 m ahead of the following sub-platoon that starts at 85 km/h. When both sub-platoons have merged, the lead sub-platoon accelerates to 80 km/h. Both sub-platoons consist of identical vehicles of 40 tonnes each and the time headway used for both sub-platoons is $\tau = 0.25\,s$. This is to analyze if the both sub-platoons can act together as one unit even when two locally centralized control are utilized.

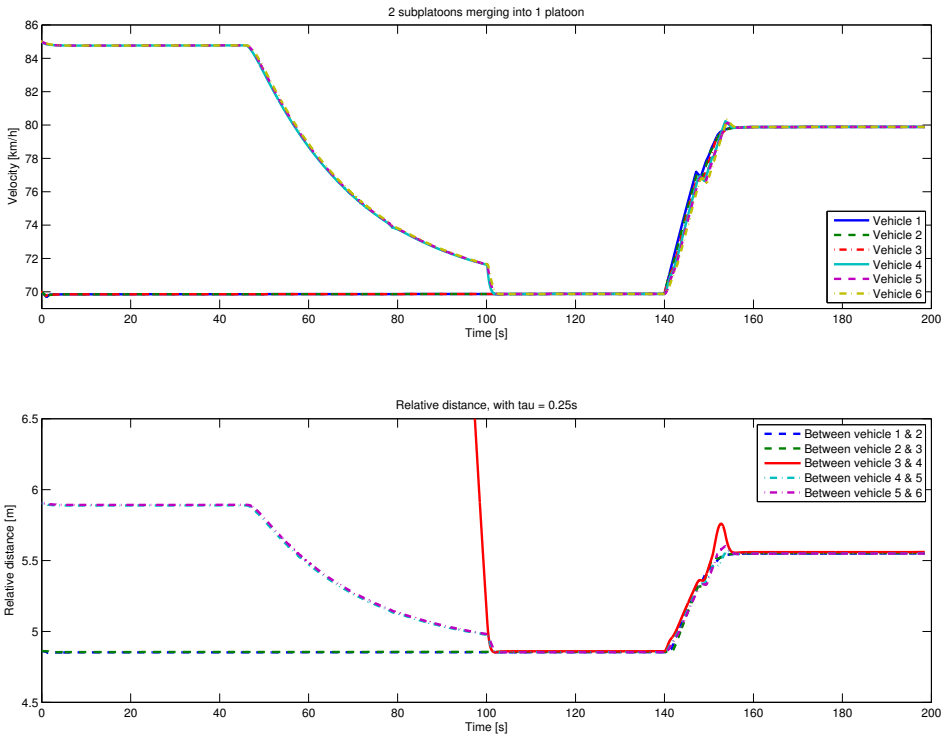

Figure 8.2: Velocity and relative distance of both sub-platoons when merging.

Figure 8.2 shows that both sub-platoons merged successfully and are acting as one long platoon even with a velocity change. The reason for a bigger distance gap at around $t = 150\,s$ is the gear shifting, which caused some acceleration loss. Therefore, the following sub-platoon had to accelerate slightly longer to make up for the distance loss. The velocity will not exceed the reference velocity set in the LQT control. Altogether, the overall performance in merging and acting as one unit is satisfying.

Part IV

Discussion

Chapter 9

Summary

9.1 String stability study with mass

The term string stability has been known for decades. With the relation that $v_i(s) = G_i^v(s)v_{i-1}(s)$, the string stability can be defined in two different ways:

$$\|G_i^v(s)\|_\infty \leq 1$$

$$\|G_2^v(s)G_3^v(s)...G_N^v(s)\|_\infty \leq 1.$$

The equations do not directly give information about the intermediate distances between the vehicles, although collisions must be prevented in platooning. Hence, a suggestion of also investigating the relative distance was proposed. The focus is to analyze how mass variations affects the string stability.

To understand the overall behavior of platooning, a simple mass-spring system was introduced: $m_i\ddot{x}_i + b_i\dot{x} = u_i$. Two transfer functions were derived, with the assumption that every vehicle in the platoon utilize the same control, a standard PID-control with respect to the difference in longitudinal position. The first function derived was the velocity transfer function $G_i^v(s)$, which did not give any further insight into string stability with mass variations. The second function derived was the relative distance transfer function $G_i^d(s)$ and by assuming three relations, an approximation was obtained. The approximated $G_i^d(s)$ holds the information on how the platoon should be arranged depending on the weight of the vehicles, namely in weight decreasing order with the heaviest vehicle first in the platoon. Simple simulations also suggest the same weight arrangement.

The issue, with utilizing the same controller with different vehicle weight, is the different dynamics each vehicle has depending on the mass. A fixed PID-control is string stable for a set of lighter vehicles up to a certain limit, where it then is no longer considered string stable. The control is rendered useless for that mass and above. Therefore, a mass depending PID-control is suggested. Algebraic derivations for both $\bar{G}_i^v(s)$ and $\bar{G}_i^d(s)$ and simulations are indicating string stable behaviors.

9.2 Locally centralized three-vehicle platoon

There already exists a decentralized control operating on vehicles, but there is no existing centralized control. Therefore, a study of a centralized control has been done, to analyze its potential possibilities in platooning.

A platoon model consisting of three HDVs is derived, from the powertrain to the external longitudinal forces. The aerodynamic drag reduction in platooning has been taken into concern in the forces acting on a HDV. The platoon model is non-linear, hence the model is linearized around an equilibrium point to enable a state-space equation.

Two LQ controls were proposed for centralized platooning. A LQR controller, where only the two last vehicles are controlled while following the lead vehicle, which is operated by the CC. A LQ tracking (LQT) controller with integral action was also proposed, which is truly a fully centralized control. The main difference between the two control laws is, that the lead vehicle does not take the following vehicles into account with LQR control while the LQT control does.

Simulations imply that both LQ controllers operate properly on a flat road and on the highway from Södertälje to Norrköping, with identical HDVs of 40 tonnes each. Different time headways were used to analyze the saved energy with safety aspects, i.e. relative distance. The results show that the reduced energy contra the time headway is almost linear. To verify how the information of the vehicle behind affects platooning, different masses were set on the second vehicle. The simulation proved the LQT controller to be better, hence staying within the platoon is more beneficial.

Lastly, it is desirable to expand the platoon to more than three vehicles. The idea is to use a switching control between the LQR and the LQT controller. Utilize the LQT control when the platoon drives independently from other platoons. When a platoon is within range, let the reference velocity slowly drop to the same velocity as the vehicle ahead. Finally, switch to the LQR control when the desired distance is achieved. This way, several sub-platoons can merge into one larger platoon and still retain the locally centralized control.

Chapter 10

Conclusion

This project was given two tasks concerning vehicle platooning. The first objective was to study the impact mass has on the robustness of a platoon, i.e. string stability. A vehicle platoon can be described as a mass-spring system and by introducing a mass difference into the system, a damping effect is instated. All types of automatic control can be described approximately as a PID-control. This turned out to be a simple analysis for string stability. Intuitively, it feels logical to have a heavier vehicle ahead. A heavier vehicle accelerates and decelerates slower and therefore, the following vehicle can easily follow the heavy vehicle and achieve a shorter braking distance. This is valid with the assumption that all the vehicle properties are identical besides the mass. Theoretical analysis and simulations confirm the same. A proposed solution to avoid a fixed mass arrangement is to introduce a mass dependent controller. This gives the possibility to obtain a string stable platoon regardless of the vehicle mass.

Given a realistic non-linear model of a HDV, the second objective was to design a centralized controller that addresses consumed energy and vehicle safety when driving in a three-vehicle platoon. A LQR control was proposed but due to the lack of a proper outer reference signal, a second control was introduced. A LQ tracking control with integral action allows an outer reference signal that enables the vehicles to follow. The difficult part was to tune the cost matrices such that a desirable performance is achieved. The focus was on the safety, to hold the correct relative distance between the vehicles. By holding a close intermediate distance, the energy consumption for the second vehicle can be reduced with $8.4 - 11.4\,\%$ depending on the set time gap and $10.5 - 13.1\,\%$ for the third vehicle when driving $80\,\mathrm{km/h}$ on a highway. This was simulated in Simulink utilizing a real road profile between Södertälje and Norrköping in Sweden. There are benefits with the LQR control despite the drawback of not having information of the following vehicles for the lead vehicle. The LQR control enables the possibility to extend longer platoons while keeping the locally centralized control properties. This is possible by introducing a switching control, which utilizes the LQT and LQR controls whenever feasible.

It is possible to obtain a smoother and comfort ride, but the reasoning was immediately dropped. A driver is driving most comfortably with a distance of several meters away on a highway. The introduction of a centralized control with a short time headway, reduces the distance to nearly a tenth. This could create comfort issues for the driver if a short time headway was utilized. The progress to a short time headway should proceed slowly for the driver to adapt. Hence, the focus was mainly to avoid vehicle collisions.

A platoon, with a LQ control, considers how each vehicle in the platoon drives and can therefore drive as one unit. A problem occurs when merging several sub-platoons. Each sub-platoons only consider their own platoon to drive as one unit, hence there is no information on the following sub-platoon, exactly like the AiCC today. This is a trade-off between quick calculations and the amount of vehicles in a sub-platoon. The proposed solution with a switching control allows fast calculations and enables the controller to remain locally centralized within the sub-platoon.

Chapter 11

Future work

There is room for further improvements with the proposed centralized controllers. Although the shortest intermediate distance proposed is 5 m at 80 km/h and the fact that a 500 ms time delay and the lowered air drag only reduce the relative distance with 2 m during hard brake, it is appropriate to analyze how the LQ controller handles time delays, noises, and package losses. Also, a switching control could cause a sudden jump or unwanted behavior to the platoon and should therefore be analyzed further.

A slight problem that occurred in this project was when the platoon was accelerating and gear shifting, a solution could be to broadcast the information that a gear shift will occur. Other information that benefit the platoon behavior should also be broadcasted. Since this project is limited to information of only velocity and distance being broadcasted, it could be an area of research to investigate what necessary information is needed for platooning.

It is possible to further decrease the consumed energy by introducing other fuel saving functions such as downhill speed control, look-ahead, and so forth. This could then be compared with a decentralized controller, such as the AiCC, and investigate the potential use for the future.

Bibliography

Assad Al Alam. Optimally fuel efficient speed adaptation. Master's thesis, Royal Institute of Technology, KTH, March 2008.

Assad Al Alam, Ather Gattami, and Karl H. Johansson. An experimental study on the fuel reduction potential of heavy duty vehicle platooning. In *2010 13th International IEEE Conference on Intelligent Transportation Systems (ITSC)*, September 2010. doi: 10.1109/ITSC.2010.5625054. ISSN: 2153-0009.

Assad Al Alam, Ather Gattami, Karl H. Johansson, and Claire J. Tomlin. Establishing safety for heavy duty vehicle platooning: A game theoretical approach. In *18th IFAC World Congress*, August 2011.

Thomas D. Gillespie. *Fundamentals of vehicle dynamics*. SAE International, February 1992. ISBN: 1-56091-199-9.

Kevin P. Groves, David O. Sigthorsson, Andrea Serrani, Stephen Yurkovich, Michael A. Bolender, and David B. Doman. Reference command tracking for a linearized model of an air-breathing hypersonic vehicle. In *Proceedings of AIAA Guidance, Navigation, and Control Conference and Exhibit*, AIAA-2005-6144, August 2005.

Gustav Hammar and Vadim Ovtchinnikov. Structural intelligent platooning by a systematic LQR algorithm. Master's thesis, Royal Institute of Technology, KTH, October 2010.

Maziar E. Khatir and Edward J. Davison. Decentralized control of a large platoon of vehicles using non-identical controllers. In *Proceedings of the 2004 American Control Conference, 2004*, June 2004. doi: 10.1109/ACC.2004.182526. ISSN: 0743-1619.

Scania CV AB. Annual report, 2001.

Michael Schittler. State-of-the-art and emerging truck engine technologies for optimized performance, emissions and life cycle costs. In *9th Diesel Engine Emissions Reduction Conference, Rhode Island, USA. U.S. Department of Energy*, August 2003.

Yoshinori Yamamura and Yoji Seto. A study of string-stable ACC using vehicle-to-vehicle communication. In *2006 SAE World Congress*, 2006-01-0348, April 2006. doi: 10.4271/2006-01-0348.

Diana Yanakiev and Ioannis Kanellakopoulos. Variable time headway for string stability of automated heavy-duty vehicles. In *Proceedings of the 34th IEEE Conference on Decision and Control, 1995*, December 1995. doi: 10.1109/CDC.1995.479245.

Diana Yanakiev and Ioannis Kanellakopoulos. A simplified framework for string stability analysis in AHS. In *In Proceedings of the 13th IFAC World Congress*, 1996.

Youping Zhang, Elias B. Kosmatopoulos, Petros A. Ioannou, and C.C. Chien. Using front and back information for tight vehicle following maneuvers. In *IEEE Transactions on Vehicular Technology*, January 1999. doi: 10.1109/25.740110. ISSN: 0018-9545.

Appendices

Appendix A

PID-controller setup

The following PID-controller setup was used in chapters 3 and 4.

$$P_i = 500\,\mathrm{N/m}, \quad I_i = 3\,\mathrm{N/ms}, \quad D_i = 20000\,\mathrm{Ns/m}$$

with $b = 172\,\mathrm{Ns/m}$ and time headway $\tau_d = 1\,\mathrm{s}$. With these values, the velocity transfer function is, which was obtained in eq. (3.6):

$$G_i^v(s) = \frac{20000s^2 + 500s + 3}{m_i s^3 + 20672s^2 + 503s + 3} \tag{A.1}$$

For the scaled-varying PID-controller, the same controller was used but together with a mass depending scalar of $K_i = \frac{m_i}{10000}$. This gives the following velocity transfer function, from eq. (4.4):

$$\bar{G}_i^v(s) = \frac{20000s^2 + 500s + 3}{10000s^3 + (\frac{1720000}{m_i} + 20500)s^2 + 503s + 3} \tag{A.2}$$

The H_∞-norms of eqs. (A.1) and (A.2) with a vehicle mass of 40 tonnes are:

$$\begin{aligned} \|G_i^v(s)\|_\infty &= 1.0029 \\ \|\bar{G}_i^v(s)\|_\infty &= 1 \end{aligned} \tag{A.3}$$

$G_i^v(s)$ is considered string unstable while $\bar{G}_i^v(s)$ is string stable according to eq. (2.2).

The simulation was done in Matlab and the scenario is from standing still to ramp from 0 to 10m/s in 10s and maintaining the speed on a flat road. Three different mass distribution were used but the total mass of the platoon remained the same to be able to make a comparison, which follows:

1. Identical vehicles, with mass of 40 tonnes each.

2. Increasing mass distribution, from 20 to 60 tonnes.

3. Decreasing mass distribution, from 60 to 20 tonnes.

The simulation was done twice with two different platoon lengths:

- Platoon length of 41 vehicles, i.e. a 1000kg weight gap between vehicles for the case with non-identical vehicles.
- Platoon length of 81 vehicles, i.e. a 500kg weight gap between vehicles for the case with non-identical vehicles.

The results of the simulations can be read in sections 3.4 and 4.2.

Appendix B

Mathematical derivation of LQR

The standard LQR cost function:

$$J^* = \min_u \int_0^{t_f} \Big(x^T(\tau) Q x(\tau) + u^T(\tau) R u(\tau) \Big) \mathrm{d}\tau + x^T(t_f) Q_f x(t_f)$$
$$\text{Subject to: } \begin{cases} \dot{x}(t) &= Ax(t) + Bu(t) \\ x(0) &= x_0 \end{cases} \tag{B.1}$$

where t_f is the time-horizon, $Q \geq 0$ is state-cost matrix, $Q_f \geq 0$ is the final state-cost matrix, and $R > 0$ is the input cost matrix. It is required that the matrix pair (A, B) is controllable.

One solution for the LQR problem is with dynamic programming. For $t \in [0, t_f]$, a value function V_t is defined by:

$$V_t(z) = \min_u \int_t^{t_f} \Big(x^T(\tau) Q x(\tau) + u^T(\tau) R u(\tau) \Big) \mathrm{d}\tau + x^T(t_f) Q_f x(t_f)$$
$$\text{Subject to: } \begin{cases} \dot{x} &= Ax + Bu \\ x(t) &= z \end{cases} \tag{B.2}$$

where $V_t(z)$ gives the minimum LQR cost-to-go, starting from state z at time t. Cost-to-go with no time left is just the final cost, hence $V_{t_f} = z^T Q_f z$ and therefore $V_0(x_0)$ is the minimum total cost. The value function is quadratic, hence the Lyapunov function is:

$$V_t(z) = z^T P_t z \tag{B.3}$$

where $P_t \geq 0$ and is symmetric. P_t can be obtained from a differential equation running backwards in time for $t \in [0, t_f]$.

By assuming that $u(t) = w$, constant over a small time interval $[t, t + h]$, the incurred cost over the interval is:

$$J_{t,t+h}(z) = \int_t^{t+h} \Big(x(\tau)^T Q x(\tau) + w^T R w \Big) \mathrm{d}\tau \approx h \left(z^T Q z + w^T R w \right) \tag{B.4}$$

and the new landed state is: $x(t+h) \approx z + h(Az + Bw)$.

Min-cost-to-go from where it lands is approximately:

$$\begin{aligned} V_{t+h}(z) &= (z + h(Az + Bw))^T P_{t+h} (z + h(Az + Bw)) \\ &\approx (z + h(Az + Bw))^T \left(P_t + h\dot{P}_t\right) (z + h(Az + Bw)) \\ &\approx z^T P_t z + h\left((Az + Bw)^T P_t z + z^T P_t (Az + Bw) + z^T \dot{P}_t z\right) \end{aligned} \tag{B.5}$$

where h^2 and higher terms were dropped. The cost-incurred together with min-cost-to-go is approximately:

$$\begin{aligned} V_t(z) &\approx V_{t+h}(z) + J_{t,t+h}(z) \\ &= z^T P_t z + h\left(z^T Q z + w^T R w + (Az + Bw)^T P_t z + z^T P_t (Az + Bw) + z^T \dot{P}_t z\right). \end{aligned} \tag{B.6}$$

By minimizing over w, the optimal input is obtained:

$$\begin{aligned} &2hw^T R + 2hz^T P_t B = 0 \\ &\Rightarrow w_{opt} = -R^{-1} B^T P_t z. \end{aligned} \tag{B.7}$$

By substituting w_{opt} from eq. (B.7) into eq. (B.6):

$$\begin{aligned} z^T P_t z &\approx z^T P_t z + h\left(z^T Q z + w^T R w + (Az + Bw)^T P_t z + z^T P_t (Az + Bw) + z^T \dot{P}_t z\right) \\ \Rightarrow\ 0 &= h\left(z^T Q z + z^T A^T P_t z + z^T P_t A^T z - z^T P_t B R^{-1} B^T P_t z + z^T \dot{P}_t z\right) \\ &= h z^T \left(Q + A^T P_t + P_t A^T - P_t B R^{-1} B^T P_t + \dot{P}_t\right) z. \end{aligned}$$

This yields to the following Riccati differential equation:

$$-\dot{P}_t = A^T P_t + P_t A^T - P_t B R^{-1} B^T P_t + Q. \tag{B.8}$$

The LQR problem can be solved using the final condition $P_{t_f} = Q_f$.

Appendix C

Mathematical derivation of LQT with integral action

With the concept of utilizing an error as: $\dot{e}_1 = r - x_1$, where r is a reference signal, an integrating action is introduced into the states as: $e_1 = \int \dot{e}_1 \mathrm{d}t$. The new state-space equation follows as:

$$\begin{bmatrix} \dot{e}_1 \\ \dot{x}_1 \end{bmatrix} = \begin{bmatrix} 0 & -I \\ 0 & A_1 \end{bmatrix} \begin{bmatrix} e_1 \\ x_1 \end{bmatrix} + \begin{bmatrix} 0 \\ B_1 \end{bmatrix} u + \begin{bmatrix} I \\ 0 \end{bmatrix} r \tag{C.1}$$

$$\Rightarrow \dot{x} = Ax + Bu + Gr.$$

The new system including the error as a state can be defined as:

$$e = \begin{bmatrix} e_1 \\ r - x_1 \end{bmatrix} = Mr + Hx. \tag{C.2}$$

The LQT cost function can now be expressed as:

$$\begin{aligned} J &= \frac{1}{2} \int_0^{t_f} \left(e^T(\tau) Q e(\tau) + u^T(\tau) R u(\tau) \right) \mathrm{d}\tau + \frac{1}{2} e^T(t_f) Q_f e(t_f) \\ \text{Subject to: } &\begin{cases} \dot{e}(t) &= HAx(t) + HBu(t) + HGr(t) \\ e(0) &= e_0 \end{cases} \end{aligned} \tag{C.3}$$

where $\dot{r} = 0$ is assumed. By inserting eq. (C.2) in eq. (C.3):

$$\begin{aligned} J &= \frac{1}{2} \int_0^{t_f} \left(x^T H^T Q H x + 2 r^T M^T Q H x + r^T M^T Q M r + u^T R u \right) \mathrm{d}\tau \\ &+ \frac{1}{2} \left(x^T(t_f) H^T Q_f H x(t_f) + 2 r^T(t_f) M^T Q_f H x(t_f) + r^T(t_f) M^T Q_f M r(t_f) \right) \end{aligned} \tag{C.4}$$

$$\text{Subject to: } \begin{cases} \dot{x}(t) &= Ax(t) + Bu(t) + Gr(t) \\ x(0) &= x_0 \end{cases}$$

where t_f is the time-horizon, $Q \geq 0$ is state-cost matrix, $Q_f \geq 0$ is the final state-cost matrix, and $R > 0$ is the input cost matrix. It is required that the matrix pair (A, B) is controllable and $H \neq 0$.

One solution for the LQT problem is by utilizing Lagrange multiplier. By introducing the Lagrange multiplier function λ and relaxing the problem by forming:

$$L = J + \int_0^{t_f} \lambda^T(\tau) \left(Ax(\tau) + Bu(\tau) + Gr(\tau) - \dot{x}(\tau) \right) \mathrm{d}\tau \tag{C.5}$$

where J is from eq. (C.4). The optimal control that minimizes eq. (C.4) will be obtained by solving the following three equations:

$$\nabla_{x(t)} L = 0 \tag{C.6a}$$
$$\nabla_{u(t)} L = 0 \tag{C.6b}$$
$$\nabla_{\lambda(t)} L = 0. \tag{C.6c}$$

Note that r is assumed to be constant. Also the state r can be seen as noise, where it is an unknown value and therefore L is not optimized and hence has no partial derivative with repsect to r.

To find a solution eq. (C.6a), the following is derived:

$$\begin{aligned} \frac{\mathrm{d}}{\mathrm{d}t} \int_0^{t_f} \lambda^T(\tau) x(\tau) \, \mathrm{d}\tau &= \int_0^{t_f} \dot{\lambda}^T(\tau) x(\tau) \, \mathrm{d}\tau + \int_0^{t_f} \lambda^T(\tau) \dot{x}(\tau) \, \mathrm{d}\tau \\ &= \lambda^T(t_f) x(t_f) - \lambda^T(0) x(0) \end{aligned}$$

$$\Rightarrow \int_0^{t_f} \lambda^T(\tau) \dot{x}(\tau) \, \mathrm{d}\tau = \lambda^T(t_f) x(t_f) - \lambda^T(0) x(0) - \int_0^{t_f} \dot{\lambda}^T(\tau) x(\tau) \, \mathrm{d}\tau. \tag{C.7}$$

By applying eqs. (C.6) and (C.7) on eq. (C.5), the following is obtained:

$$\nabla_{x(t)} L = 0 = H^T Q H x + H^T Q M r + A^T \lambda + \dot{\lambda} \tag{C.8a}$$
$$\nabla_{u(t)} L = 0 = Ru + B^T \lambda \quad \Rightarrow \quad u = -R^{-1} B^T \lambda \tag{C.8b}$$
$$\nabla_{\lambda(t)} L = 0 = Ax + Bu + Gr - \dot{x}. \tag{C.8c}$$

Equation (C.8c) is the dynamical system, which must always be satisfied. From $\nabla_{x(t_f)} L$, the following final condition is obtained:

$$\begin{aligned} \nabla_{x(t_f)} L = H^T Q_f H x(t_f) + H^T Q_f M r(t_f) - \lambda(t_f) = 0 \\ \Rightarrow \lambda(t_f) = H^T Q_f H x(t_f) + H^T Q_f M r(t_f). \end{aligned} \tag{C.9}$$

By adding the Lagrange multiplier as a state, from eq. (C.8a), to the dynamic linear system and replacing u described in eq. (C.8b), the new system with the final condition from eq. (C.9) can be described as:

$$\begin{aligned} \begin{bmatrix} \dot{x} \\ \dot{\lambda} \end{bmatrix} &= \begin{bmatrix} A & -BR^{-1}B^T \\ -H^TQH & -A^T \end{bmatrix} \begin{bmatrix} x \\ \lambda \end{bmatrix} + \begin{bmatrix} G \\ -H^TQM \end{bmatrix} r \\ \text{Subject to:} &\begin{cases} x(0) = x_0 \\ \lambda(t_f) = H^TQ_fHx(t_f) + H^TQ_fMr(t_f). \end{cases} \end{aligned} \tag{C.10}$$

The new conditions are known as a two-point boundary value problem. Similar with the case of LQR problem, the solution can be calculated backwards, from the final condition to initial condition. The Lagrange multiplier solution can be given asserted as follow:

$$\lambda = P_tx + g_tr. \tag{C.11}$$

By inserting this into the second state in eq. (C.10):

$$\dot{\lambda} = \dot{P}_tx + P_t\dot{x} + \dot{g}_tr = -H^TQHx - A^T\lambda - H^TQMr$$

whereas $\dot{x}$ is known and gives the following equation:

$$\begin{aligned} \dot{P}_tx + P_tAx - P_tBR^{-1}B^TP_tx - P_tBR^{-1}B^Tg_tr + P_tGr + \dot{g}_tr = \\ = -H^TQHx - A^TP_tx - A^Tg_tr - H^TQMr. \end{aligned}$$

Given that $x \neq 0$ and $r \neq 0$, this yields to two differential equations:

$$\dot{P}_t = -P_tA^T - A^TP_t - H^TQH + P_tBR^{-1}B^TP_t \tag{C.12a}$$

$$\dot{g}_t = (P_tBR^{-1}B^T - A^T)g_t - (H^TQM + P_tG) \tag{C.12b}$$

that must be satisfied. Equation (C.12a) is the standard Riccati differential equation and eq. (C.12b) is an auxiliary vector equation defining the feedforward gain. The LQT problem can be solved using the final conditions:

$$\begin{aligned} P_{t_f} &= H^TQ_fH \\ g_{t_f} &= H^TQ_fM. \end{aligned}$$